

HYDROTHERMAL CARBONIZATION CARBON-BASED ACID CATALYST FOR BIODIESEL PRODUCTION



A Dissertation Submitted in Partial Fulfillment of the Requirements
for the Degree of Doctor of Engineering in Chemical Engineering
Department of Chemical Engineering
Faculty of Engineering
Chulalongkorn University
Academic Year 2018
Copyright of Chulalongkorn University

ตัวเร่งปฏิกิริยากรดจำพวกคาร์บอนจากกระบวนการไฮโดรเทอร์มอลคาร์บอนในเซชัน เพื่อการ
ผลิตไบโอดีเซล



วิทยานิพนธ์นี้เป็นส่วนหนึ่งของการศึกษาตามหลักสูตรปริญญาวิศวกรรมศาสตรดุษฎีบัณฑิต
สาขาวิชาวิศวกรรมเคมี ภาควิชาวิศวกรรมเคมี
คณะวิศวกรรมศาสตร์ จุฬาลงกรณ์มหาวิทยาลัย
ปีการศึกษา 2561
ลิขสิทธิ์ของจุฬาลงกรณ์มหาวิทยาลัย

ศักดิ์วาลย์ คุมโคตร : ตัวเร่งปฏิกิริยากรดจำพวกคาร์บอนจากกระบวนการไฮโดรเทอร์มอลคาร์บอนในเซชัน เพื่อ
การผลิตไบโอดีเซล. (HYDROTHERMAL CARBONIZATION CARBON-
BASED ACID CATALYST FOR BIODIESEL PRODUCTION) อ.ที่ปรึกษา
หลัก : ศ. ดร.อาทิวรรณ โชติพฤษย์

งานวิจัยนี้เป็นการศึกษาการผลิตไบโอดีเซล (โอเลอิกเมทิลเอสเทอร์) จากปฏิกิริยาเอสเทอร์ริฟิเคชันในระบบที่มี
ตัวเร่งปฏิกิริยาชนิดซัลโฟเนตเต็ดไฮโดรเทอร์มอลคาร์บอนภายใต้ความร้อนระบบไมโครเวฟ โด ย ตัวเร่งปฏิกิริยาชนิดซัลโฟ
เนตเต็ดไฮโดรเทอร์มอลคาร์บอน ถูกเตรียมจากกระบวนการไฮโดรเทอร์มอลคาร์บอนในเซชัน และติดหมู่ซัลโฟนิกผ่านกระบวนการ
การซัลโฟเนชันตามลำดับ ตัวเร่งปฏิกิริยา ชนิดซัลโฟเนตเต็ดไฮโดรเทอร์มอลคาร์บอน มีจุดอ่อนไวในการเกิดปฏิกิริยาที่กรด
ซัลโฟนิก ซึ่งได้รับการยืนยันว่าเป็นตัวดูดซับคลื่นไมโครเวฟที่ดี โดยสามารถเกิดความร้อนได้อย่างรวดเร็วทำให้เร่งปฏิกิริยาได้
ทันทีที่ผิวของตัวเร่งปฏิกิริยาการศึกษาสภาวะที่เหมาะสมของปฏิกิริยาเอสเทอร์ริฟิเคชันระหว่างกรดโอเลอิกและเมทานอลถูก
ออกแบบด้วยวิธีการวิเคราะห์พื้นผิวดูดซับแบบการออกแบบส่วนประสมกลางเซลล์ทรีลอมโพสิต ตัวแปรในการศึกษาได้แก่
อัตราส่วนโดยโมลของกรดโอเลอิกกับเมทานอล (1:2.5-1:7.5) เวลาในการทำปฏิกิริยา (50-70 นาที) และปริมาณ
ตัวเร่งปฏิกิริยา (2-5 ร้อยละน้ำหนักโดยมวล) จากการศึกษาพบว่า ตัวแปรอิสระที่มีผลต่อปฏิกิริยามากที่สุดคือ อัตราส่วนโดย
โมลของกรดโอเลอิกกับเมทานอล ตามมาด้วยปริมาณตัวเร่งปฏิกิริยา ในขณะที่ เวลาในการทำปฏิกิริยา ไม่มีผลอย่างมีนัยสำคัญ
ในช่วงของการศึกษา แบบจำลองทางสถิติทำนายสภาวะที่เหมาะสมให้ผลิตภัณฑ์ไบโอดีเซลร้อยละ 95.55% ที่อัตราส่วนโดย
โมลของกรดโอเลอิกกับเมทานอลเท่ากับ 1:5.8 เวลาในการทำปฏิกิริยา 60 นาทีและปริมาณตัวเร่งปฏิกิริยาเท่ากับ3.05 ร้อย
ละน้ำหนักโดยมวล ผลการทดลองจึงยืนยันว่าแบบจำลองทางสถิติมีความน่าเชื่อถือ ด้วยค่าสัมประสิทธิ์การถดถอย 0.9407
โดยมีค่าความผิดพลาดในการทำนายจากแบบจำลองเพียงร้อยละ 2.79 นอกจากนี้การศึกษาดนพลศาสตร์ทางเคมีของปฏิกิริยา
นี้พบว่าเป็นปฏิกิริยาอันดับหนึ่งเหมือน โดย ค่าคงที่ของอัตราการเกิดปฏิกิริยาขึ้นอยู่กับอุณหภูมิ และมีค่าพลังงานกระตุ้นเท่ากับ
64 กิโลจูลต่อโมล นอกจากนี้ ยังศึกษาความเป็นไปได้ในการนำ ตัวเร่งปฏิกิริยาชนิดซัลโฟเนตเต็ดไฮโดรเทอร์มอลคาร์บอนที่
ผ่านการใช้งานแล้ว กลับมาใช้ซ้ำ พบว่ามีการเสื่อมสภาพอย่างรวดเร็วหลังการนำกลับมาใช้ซ้ำครั้งแรก ซึ่งปัญหาดังกล่าวสามารถ
แก้ไขได้โดยการปรับปรุงวิธีการเตรียมตัวเร่งปฏิกิริยาให้มีความเสถียรมากขึ้น

จุฬาลงกรณ์มหาวิทยาลัย
CHULALONGKORN UNIVERSITY

สาขาวิชา วิศวกรรมเคมี
ปีการศึกษา 2561

ลายมือชื่อนิสิต

ลายมือชื่อ อ.ที่ปรึกษาหลัก

5571452521 : MAJOR CHEMICAL ENGINEERING

KEYWOR

D:

Laddawan Tumkot : HYDROTHERMAL CARBONIZATION CARBON-BASED ACID CATALYST FOR BIODIESEL PRODUCTION. Advisor: Prof. ARTIWAN SHOTIPRUK, Ph.D.

This study aims to synthesize the production of biodiesel (oleic acid methyl ester) by esterification in the presence of sulfonated hydrothermal carbon based catalyst under microwave irradiation. The catalyst was prepared by hydrothermal carbonization, followed by sulfonation presenting sulfonic acid group as an active site. The catalyst characterization results confirmed good microwave-absorptivity of the catalyst which can be heated directly and accelerate the reaction immediately at the surface of the catalyst. Esterification of oleic acid (OA) with methanol experiments were optimized by using response surface methodology based on central composite design. Three variables: molar ratio of methanol to OA (2.5:1–7.5:1), reaction time (50-70 min) and catalyst loading (2-5 wt%) were studied. The results indicated that molar ratio of methanol to OA was the most influential factor on OA conversion and followed by catalyst loading. While, the reaction time showed negligible effect on OA conversion within the range studied. Based on the model, the optimum OA conversion of 95.55% was predicted at 5.8:1 methanol to OA molar ratio, 60 min and 3.05 wt% catalyst loading. The experimental validation carried out at this condition indicated that the model gave good prediction of OA conversion, with only 2.79% error and the coefficient of regression (R^2) of 0.9407. Furthermore, the reaction was found to be reasonably described by the pseudo-first order kinetics. The dependency of the reaction rate constant on temperatures gave the value of the activation energy of 64 kJ/mol. Moreover, the effect of catalyst recycling was studied. The decrease in OA conversion is significant according to the catalyst is not active after first run. As a result, the deactivation can be solved by improving the stability of the catalyst.

Field of Study: Chemical Engineering

Student's Signature

Academic 2018

Advisor's Signature

Year:

.....

ACKNOWLEDGEMENTS

It is my proud privilege to release the feelings of my gratitude to several persons who helped me directly and indirectly to conduct this research project work. This thesis would not have been possible without the help, guidance and support from my supervisor, Prof. Artiwan Shotipruk. I would like to express my deep sense of thanks and gratitude for her patience and unfailing faith all the way through my research work from the beginning.

Respectful thanks are offered to Prof. Tetsuya Kida, Prof. Armando T. Quitain and Assoc. Prof. Mitsuru Sasaki for their warm regards during my exchange stay in Kumamoto University, Japan.

Special thanks to all of my thesis committees, Prof. Suttichai Assabumrungrat, Prof. Sarawut Rimdusit, Prof. Navadol Laosiripojana and Dr. Chalida Klaysommade for their useful guidance and recommendations which made this thesis come to completion.

I am grateful to Dr. Panatpong Boonnoun for his precious time, kind advice, motivation and helpful suggestion on my research.

I would like to acknowledge the financial, academic and technical support of 60/40 Chulalongkorn Scholarship, e-ASIA Joint Research Program and Japan Student Services Organization (JASSO) Scholarship.

I am thankful to all my friends and members both of the Biochemical Engineering Research Laboratory, Department of Chemical Engineering, Chulalongkorn University and Department of Applied Chemistry and Biochemistry, Kumamoto University for their assistance, warm collaborations and friendly encouragement.

Finally, to my parents and my family, I won't be stronger without you as my inspiration. I take this opportunity to express my greatest gratitude to for their understanding, support, blessings, encouragement, and infinite love which were the sustaining factors in carrying out the work successfully.

Laddawan Tumkot

TABLE OF CONTENTS

	Page
ABSTRACT (THAI)	iii
ABSTRACT (ENGLISH).....	iv
ACKNOWLEDGEMENTS.....	v
TABLE OF CONTENTS.....	vi
CHAPTER I.....	9
INTRODUCTION	9
1.1 Motivation.....	9
1.2 Objectives	11
1.3 Working scopes	12
1.4 Expected benefits.....	12
CHAPTER II.....	13
BACKGROUND AND LITERATURE REVIEWS	13
2.1 Biodiesel	13
2.1.1 The production of biodiesel.....	13
2.1.2 Catalysts for biodiesel production.....	16
2.1.3 The alternative microwave heating	25
2.2 Design of experiment.....	30
2.3 Kinetic study.....	36
CHAPTER III	38
MATERIALS AND METHODS	38
3.1 Materials and chemicals	38
3.2 Preparation and characterization of hydrothermal carbon-based acid catalyst (S-HTC).....	38
3.2.1 Hydrothermal carbon (HTC) preparation.....	38
3.2.2 Acid functionalized hydrothermal carbon preparation.....	39
3.3 Esterification of OA with methanol.....	41

3.3.1 Catalytic activity.....	41
3.3.2 Optimization study	43
3.3.2.1 Screening parameters effect	43
3.3.2.2 Design of experiment, analysis and model fitting.....	43
3.3.3 Kinetics study of S-HTC catalyzed esterification	44
3.3.4 Reusability of S-HTC on esterification	46
CHAPTER IV	47
RESULTS AND DISSCUSSION.....	47
4.1. S-HTC characterization	47
4.2. Catalytic activity of S-HTC on esterification reaction	50
4.2.1 Screening parameters effect	50
4.2.2 A single variable study	52
4.2.2.1 Effect of reaction temperature and time	52
4.2.2.2 Effect of molar ratio of oleic to methanol	53
4.2.2.3 Effect of catalyst loading.....	54
4.2.2.4 Effect of amount of hexane	55
4.3 Optimization of S-HTC catalyzed OA esterification conditions.....	56
4.3.1 Screening variables affecting OA esterification.....	56
4.3.2. Design of experiment, quadratic regression model and variance analysis	58
4.3.3. Effect of variables on OA conversion	61
4.3.4. Optimization of OA conversion	62
4.4. Kinetics study of S-HTC catalyzed esterification	65
4.4.1. Determination of kinetic parameters	65
4.4.2. Arrhenius plot and activation energy	66
4.5. Stability, reusability and spent catalyst characterization of S-HTC	67
CHAPTER V	69
CONCLUSIONS AND RECOMMENDATIONS	69
5.1 Conclusions.....	69

5.2 Recommendations.....	70
APPENDIX A.....	72
EXPERIMENTAL DATA FOR ANALYSIS	72
A1 Standard calibration curve	72
A2 Calculation of the OA conversion	74
APPENDIX B	75
EXPERIMENTAL DATA.....	75
B1 Catalytic activity	75
B2 Screening parameters effect	75
B3 Design of experiment	77
B4 Kinetics study.....	78
B5 Reusability	78
REFERENCES	79
VITA.....	95
REFERENCES	96
VITA.....	98

CHAPTER I

INTRODUCTION

1.1 Motivation

Owing increasing global environment concerns, biodiesel or fatty acid methyl ester (FAME) being biodegradable fuel produced from renewable raw materials such as vegetable oils and animal fats, is one of the most promising alternative energies that have received much attention worldwide a current promising. It has good combustion, low toxicity and compatible with conventional diesel (Ye et al., 2016; Jiang et al., 2013; Hashemzahi et al., 2017). Considering the economic issue of biodiesel production process, raw materials and catalysts are two main contributing factors to the overall cost of biodiesel (Chuah et al., 2017; Mardhiah et al., 2017; Trombettoni et al., 2018). With this regard, low-cost feedstocks, such as oils high in free fatty acids (FFAs), are more cost effective raw materials for commercial biodiesel production through esterification reaction. While homogeneous acid catalysts (H_2SO_4 , H_3PO_4 and HCl) are commonly used to catalyze this reaction, environmental concerns and problems with equipment corrosion have led to development of new green catalysts (Zhang et al., 2016).

Carbon-based catalysts have been gaining attention owing to their high acid density and thermal stability, the use of low-cost carbon sources as raw material, as well as the simple synthesis route. The major drawback of this catalyst is on the preparation as the conventional pyrolysis/carbonization method involves working on high temperature (400-800°C). The hydrothermally synthesized carbonaceous materials, called hydrothermal carbon (HTC), reported by Titirici, et al. (2008), from which the preparation process takes place in water at lower temperatures (150-250°C), is an interesting carbon material. Besides, the HTC can be functionalized with a specific active site for a particular reaction, namely sulfonic acid, phosphate, polycyclic aromatic, polyethyleneimine, imidazole, and so on (Fraile et al., 2012; Fan et al., 2013; Egres et al., 2019; Atta-Obeng et al., 2018; Demir-Caken et al., 2010). Zhang et al. (2016) observed a good reusability with the high catalytic performance toward the esterification of sulfonated carbon-based solid acid microspheric material

prepared by hydrothermal method after 6 uses. However, slow rate reactions are reported in heterogeneous catalytic reactions. Accordingly, a rapid heating on a molecular basis is interesting as a heat directly to the selective materials and to accelerate the reaction rate as mentioned above.

Microwave (MW) heating is the alternative heating source which provides internal heating on a molecular basis of the selective materials. Previously, MW has been widely applied in several chemical reactions. Since heat is directly to the selective materials with advantages of rapid and uniform heating, short reaction time and energy savings (Menéndez et al., 2010; Mazo et al., 2012; Motasemi & Ani, 2012; Ma et. Al., 2016; Prommuak et al., 2016; Hashemzahi et al., 2017). Within the MW field, MW absorbing materials orient and align themselves according to the direction of the electric field with the same frequency with the MW (i.e. at MW frequency of 2.45 GHz, the molecule alternate the direction 2.45 billion times per second). As a result, heat is generated from the loss of energy through molecules friction. The direct heating of the materials on a molecular basis leads to rapid heat. The ability of materials to be heated under MW is determined by the dielectric loss tangent, $\tan \delta$, which is defined as the dielectric constant (ϵ''), which determines the conversion of electrical energy into heat divided by the dielectric loss factor (ϵ'), which describes the capability of the materials for energy storage in the electric field. The different carbonaceous materials such as activated carbon, charcoal and carbon nanotube were found to be a good MW absorber with the range of 0.11-0.80 dielectric loss tangent at 2.45 GHz and 298 K compare to the loss tangent of distilled water (0.118) at the same condition (Menéndez et al., 2010). Therefore, under MW heating, the carbon materials play double roles of catalyst and MW absorber contributing to heterogeneous catalytic reactions.

Regarding to a reversible reaction of esterification, either ways for shifting the position of equilibrium to the right side according to Le Chatelier's principle are adding an excess reactant or/and removing one of the product. An excess alcohol (methanol is most widely used) is usually used in order to achieved higher conversion efficiency in the reaction. Moreover, the addition of hexane in the proposed process will further drive higher yields since the product could be immediately removed from

the reaction mixtures. Besides, being non-polar, it is microwave transparent and would not add up to the energy requirement for the reaction. Another benefit of this non-polar characteristic of hexane is the ability to separate FAME from the reaction mixture whereby FAME is soluble in non-polar phase. When FAME could be separated from the reaction zone right after it is produced the yield is expected to be higher due to the forward shift in equilibrium.

Owing to the ability of the sulfonated HTC (S-HTC) and methanol in absorbing MW energy and dissipating it into heat ($\tan \delta=0.196$ and $\tan \delta = 0.659$, respectively, at 2.45 GHz and 298 K), in this work, esterification of OA with methanol catalyzed with S-HTC in the system with and without hexane was investigated under microwave irradiation. Optimization of the reaction condition was conducted using response surface methodology (RSM) with a central composite design (CCD) to evaluate the effect of each variable and the variable interaction via quadratic model. The statistical model was proposed and was experimentally validated at the suggested optimum condition. Moreover, kinetic study of OA esterification was performed to determine the kinetic parameters important for future process design, including the reaction rate constants at different temperatures, the activation energy and the pre-activation energy.

1.2 Objectives

1.2.1 To test the catalytic activity of S-HTC on esterification of OA and methanol under microwave irradiation.

1.2.2 To evaluate the effect of hexane to the esterification reaction.

1.2.3 To screen parameters affecting S-HTC catalyzed esterification conditions.

1.2.4 To optimize esterification conditions catalyzed by S-HTC under microwave irradiation using response surface methodology (RSM) with a central composite design (CCD).

1.2.5 To determine kinetic parameters of esterification promoted by S-HTC.

1.2.6 To study the reusability of S-HTC in esterification.

1.3 Working scopes

1.3.1 Evaluating the effect of hexane to methanol amount (H/M = 0, 0.5, 1, 1.5, 2 v/v)

1.3.2 Screening the effect of parameters of molar ratio of oleic acid to methanol (1:1, 1:5, 1:10, 1:20), reaction time (15, 30, 45, 60 min) and catalyst loading (0, 1, 2.5, 5, 10 wt%) on the esterification reaction under microwave irradiation.

1.3.3 Design of experiment of esterification using CCD at 3 levels: low, middle and high, designated as -1, 0 and +1 respectively in 17 experimental runs: 8 factorial points, 6 axial points and 3 replicates at the center point.

1.3.4 Determine kinetic parameters in the temperature range of 70-100°C under the optimized condition for 0, 15, 30, 45 and 60 min.

1.3.5 Evaluate the performance of recycling S-HTC in esterification.

1.4 Expected benefits

1.4.1 Successfully conducted carbon-based acid catalyst by using green and environmental friendly method on esterification reaction for biodiesel production.

1.4.2 Prediction and optimization OAME conversion via RSM based on CCD.

CHAPTER II

BACKGROUND AND LITERATURE REVIEWS

2.1 Biodiesel

Renewable energies have received much attention, owing to high price of petroleum and global environment concerns. Biodiesel or fatty acid methyl ester (FAME) is a current promising biodegradable fuel, which can be produced using renewable sources as raw materials e.g. vegetable oils and animal fats. It has good combustion, low toxicity and compatible with conventional diesel (Liu et al., 2013; Jiang et al., 2013). Considering the economic issue of biodiesel production process, raw materials and catalysts are two main contributing factors that increase the overall cost of biodiesel production (Chuah et al., 2017; Mardhiah et al., 2017; Trombettoni et al., 2018).

2.1.1 The production of biodiesel

There are four methods for biodiesel production: direct use, microemulsions, thermal cracking and transesterification. Direct use of vegetable oil (20%) and blending with diesel fuel (80%) was successful at the beginning in 1980 and carried out using up to 50/50 ratio. But, it is not applicable to most of actual engines due to high viscosity and low flash point (Harwood, et. al., 1984; Ma et al., 1999). Microemulsion is an approach method for reducing viscosity by microemulsification with short chain alcohol. The pseudo ternary phase equilibrium was used to identify the suitable formulation of single phase of mixture as shown in Figure 2.1. However, low heating values and low cetane numbers are the main problem leading to incomplete combustion.

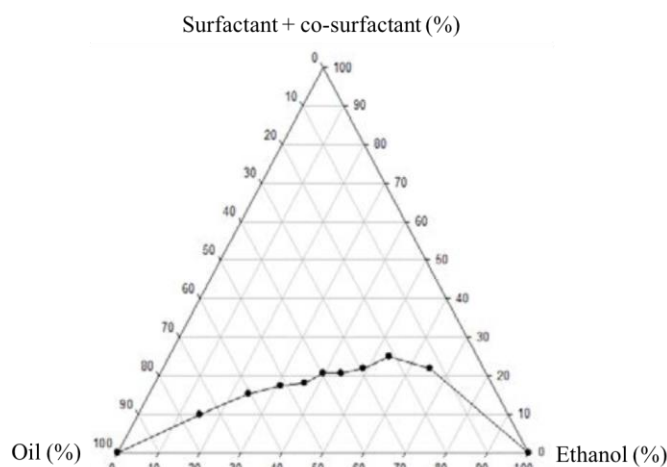


Figure 2.1 Microemulsion biofuel phase diagram (Ekkpowpan P. et al., 2014).

Thermal cracking (pyrolysis) is a decomposition of complex structure of hydrocarbons into smaller molecules at high temperature (550-850°C) with or without catalyst. High temperature leads to high yield of light hydrocarbons as shown in Table 2.1 (Billaud et al., 1995) and also leads to be supported by suitable equipment which is expensive.

Table 2.1 Selectivity of cracking products as a function of pyrolysis temperature

	Selectivity (molar % of carbon atoms cracked)						
	550°C	600°C	650°C	700°C	750°C	800°C	850°C
C ₁ -C ₄ cut	10.0	18.6	28.2	38.7	35.1	45.1	66.1
C ₅ -C ₉ cut	36.0	19.6	17.6	13.2	17.5	12.6	3.6
C ₁₀ -C ₁₄ cut	3.0	3.5	3.5	2.7	1.7	1.0	0.3
C ₁₅ -C ₁₈ cut	0.9	0.7	0.3	1.1	0.3	0.2	0.3
Aromatics	5.2	2.0	2.7	3.9	7.2	11.6	8.9
C _{3:1} -C _{8:1} esters	8.5	16.6	10.3	7.2	5.9	4.1	0.9
C _{9:1} -C _{16:1} esters	2.3	3.2	3.4	2.3	0.9	0.5	0.3
Saturated esters	2.0	1.2	1.6	2.4	3.7	3.1	2.6
CO	0.5	1.2	1.3	2.3	2.7	3.8	5.3
CO ₂	0.3	0.6	0.6	1.1	1.5	1.6	2.1
Coke	6.1	3.8	4.2	4.7	2.2	3.1	4.5
Other products	25.2	29.0	25.3	20.4	21.3	13.3	5.1
Selectivity (molar % of hydrogen atoms cracked)							
H ₂	0.3	0.9	1.7	2.7	3.6	4.6	5.9

The most common method for biodiesel production is trans-esterification (also known as alcoholysis). The triglycerides and alcohols are the requirement reactants for this reaction. The overall reaction is shown in Figure 2.2. R₁, R₂ and R₃ of the triglycerides are long chain hydrocarbon constituting fatty acids which maybe the

same or different. The three stepwise reactions of triglyceride are converted to diglyceride and monoglyceride intermediate respectively, and finally to glycerol (Rubi R. et al., 2012).

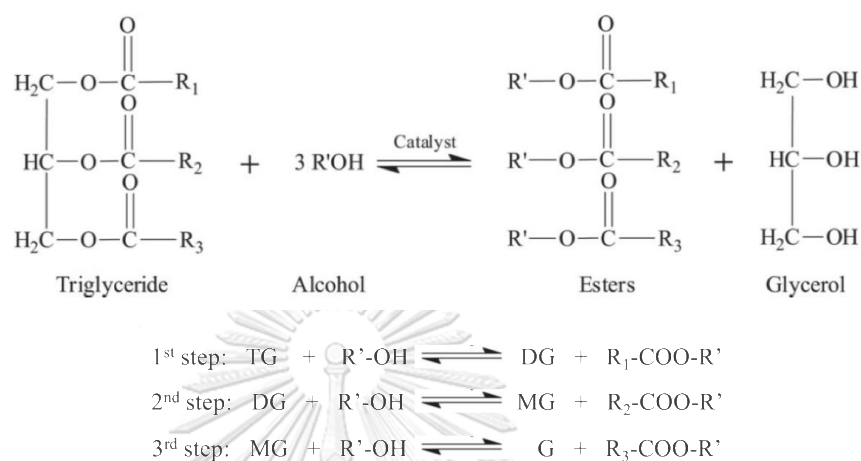


Figure 2.2 Transesterification of triglyceride

Methanol is the preferable alcohol in this reaction owing to the small alkyl group and easy attachment exchanging of ester compound. The reaction is reversible but the back reaction is negligible because an excess of alcohol is usually employed to force reaction towards the right side (Meher et al., 2006). The stoichiometry of reaction is a 3:1 molar ratio of alcohol to oil, to produce 3 mol of biodiesel and 1 mol of glycerol. Though, in practice it is usually increased from 6:1 to 1000:1 to favor the formation of products and increase its performance. The transesterification is favored to catalyze using homogeneous and heterogeneous alkaline catalysts such as NaOH, KOH, CaO, Calcium ethoxide, KOH/NaX Zeolite (Leung et al., 2006; Rashid et al., 2008; Nui et al., 2014; Xie et al., 2017]. Unfortunately, the alkaline catalyst is not appropriate for high free fatty acid (FFAs) due to soap formation. If FFA exist in the feedstock, acid catalyst is used to catalyze carboxylic acid and alcohol to produce ester form. The reaction is called esterification which is the subset of transesterification. The reaction is shown in Figure 2.3.

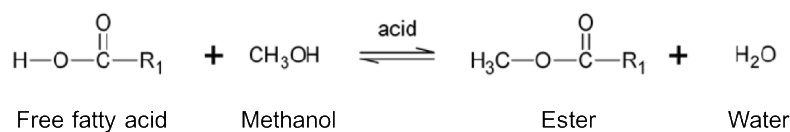


Figure 2.3 Esterification of free fatty acid

2.1.2 Catalysts for biodiesel production

The catalytic for biodiesel production can be classified as non-catalytic, bio-catalytic and chemical catalytic. Non-catalytic as known as supercritical alcohol operates at temperature and pressure in excess of its critical point to exhibit unusual properties. First, the polarity of alcohol decreases with increasing temperature to hydrophobic nature in supercritical state. A single fluid phase is formed without mass transfer limitation between phases of reactants. Second, a hydroxyl group from primary alcohol takes on the properties of super-acids so the reaction can be produced FAME without catalyst. However, the requirement of high temperature (230-450°C), high pressure (19-60 MPa) and large amount of methanol (40-45:1 molar ratio of methanol to oil) are limited for industrial scale (Saka et al., 2001). While bio-catalytic or enzymatic production of biodiesel can be carried out at mild temperature and atmospheric pressure. Moreover, it is not sensitive to FFA and water content in feedstock (Zullaikah et al., 2005). Enzyme catalyst is a clean biofuel production with low environmental impact due to no byproduct generation. But, the main problem of this method concerns with enzyme stability, recovery and the high cost of immobilization enzyme.

Conventionally, biodiesel is produced using chemical catalysts (acidic and basic). Catalysts can be classified as homogeneous and heterogeneous catalysts. Homogeneous catalyst is in the same phase as the reaction mixture, whereas heterogeneous catalyst is in a different phase of reactant(s). Unfortunately, the homogeneous catalysts suffer from many drawbacks including corrosive, harmful and waste treatment after washing process (Liu. et al., 2013; Zhang et al., 2012). Therefore, heterogeneous catalyst has been gaining attention for replacement conventional homogeneous catalyst due to ease of separation and reusable. Heterogeneous acid and basic catalysts used in biodiesel production are shown in

Table 2.2 and Table 2.3, respectively. In general, solid base catalysts are more active than solid acid catalysts in transesterification reaction regarding of mild reaction conditions and shorter reaction time. However, high FFAs and moisture content of feedstock are necessary to consider because the alkali catalyst reacts with FFAs to form soap and water also hydrolyzes the triglycerides into diglycerides and monoglycerides which is more FFAs. Free fatty acids esterification reaction is an alternative process to transesterification when low-cost feedstocks with high FFAs are used. Although esterification reaction is reversible reaction, the equilibrium can be shifted to produce more FAME either by adding an excess a reactant (usually methanol) or by removing one of the product. For batch system, the non-polar solvent (hexane) is used to separate FAME from the reaction mixture whereby FAME is soluble in non-polar phase. When FAME could be separated from the reaction zone right after it is produced the yield is expected to be higher due to the forward shift in equilibrium. Moreover, acid catalysts are used to overcome the slow reaction rate of esterification. There are many acid solids catalyzed esterification such as metal (zirconium, titanium, tin oxide, tungsten) oxide, sulfonic ion exchange resin, sulfonic modified mesostructure silica and heteropolyacids (HPAs) (Lam et al., 2010). Generally, high reaction temperatures are required to carry out FAME through esterification reaction as shown in Table 2.4. The commercial acid catalyst, Amberlyst, not only has a limitation of using at high temperature (<110 °C) due to their stability of resin but also expensive for industrial process.

Recently, carbon-based catalyst has been gaining attention caused by low-cost carbon sources as well as simple synthesis route to get high acid density and thermal stability. The preparation process of carbonaceous materials for synthesizing carbon-based catalysts are dehydration and carbonization, which can be achieved conventionally by incomplete carbonization/pyrolysis (400-800 °C). Then carbonaceous materials can be functionalized with a specific active site for a particular reaction, namely sulfonic acid, phosphate, polycyclic aromatic, polyethyleneimine, imidazole, and so on (Fraile et al., 2012; Fan et al.; 2013, Egres et al.; 2019, Atta-Obeng et al.; 2018, Demir-Caken et al., 2010) as shown in Figure 2.4.

Table 2.2 Summary of the activity and reaction conditions of various types of heterogeneous acid catalysts used in biodiesel production

Catalyst	Preparation method	Characterization	Feedstock	Type of alcohol (alcohol to oil molar ratio)	Catalyst loading (wt%)	Temperature (°C)	Reaction time (h)	Performance	Ref.
Mixed oxides WO ₃ /ZrO ₂	ZrO ₂ impregnated with ammonium metavanadate hydrate	SSA = 57 m ² /g	Vegetable oils	Methanol (19.4:1)	0.2 g	75	140	70% conversion of FFA	Park et al., 2010
TiO ₂ /SO ₄ ²⁻	TiO ₂ ·nH ₂ O was precipitated from TiCl ₄ by aq. NH ₃ ; immersed in H ₂ SO ₄ and calcined at 550°C for 3 h	SSA = 230 m ² /g	Cottonseed oil	Methanol (12:1)	2	230	8	90% yield	Chen et al., 2006
Al ₂ O ₃ /TiO ₂ /ZnO	Boehmite was co-mixed with titanium gel and ZnO in HNO ₃ and H ₂ O and calcined at 600°C for 3 h	SSA = 62 m ² /g	Colza oil	Methanol (1:1)	6	200	8	93.7% yield	B. Delford et al.*
Zeolites and zeotypes									
H ⁺ ion exchanged ZSM-5	synthetic mixture of colloidal silica, aluminum hydroxide, potassium hydroxide and deionized water were reacted hydrothermally, aged 72 h and heated at 190°C for 48 h. Calcination was at 550°C for 6 h	BET surface area = 413 m ² /g	Soybean oil	Methanol (5:1)	0.5	60	1	80% conversion	Chung et al., 2009
Mordenite zeolite	Commercial MOR zeolites were washed with deionized water, dried at 100°C calcined at 500°C for 12 h	BET surface area = 419 m ² /g	Soybean oil	Methanol (5:1)	0.5	60	1	80% conversion	Chung et al., 2009
H-type faujasite zeolites	2 M NH ₄ NO ₃ solution at 80°C was used for ion exchange on Na-type FAU zeolite, filtered, washed and dried for 12 h at 100°C and calcined at 550°C for 5 h	BET surface area = 574 m ² /g	Soybean oil	Methanol (5:1)	0.5	60	1	75% conversion	Chung et al., 2009
Heteropoly acids and Polyoxometalates									
Zirconia supported HPA	Zirconyl chloride solution was hydrolyzed and dried for 12 h at 120°C, powdered and dried for 12 h, calcined at 750°C for 4 h	SSA = 70 m ² /g	Sunflower Mustard	Methanol (20:1)	3	200	5	97% conversion	Sunita et al., 2008

Table 2.2 (continued)

Catalyst	Preparation method	Characterization	Feedstock	Type of alcohol (alcohol to oil molar ratio)	Catalyst loading (wt%)	Temperature (°C)	Reaction time (h)	Performance	Refs.
H ₃ PW ₁₂ O ₄₀ ·6H ₂ O	Catalyst was calcined at 119.85°C	Not reported	Water was adsorbed simultaneously by 4 A zeolite	Methanol (70:1)	3.7	65	14	87% yield	F. Cao et al.*
C _{3.5} H _{0.5} PW ₁₂ O ₄₀	An aqueous solution of C ₃ CO ₃ was added drop-wise to an H ₃ PW ₁₂ O ₄₀ ·19H ₂ O solution under vigorous stirring at room temperature overnight	Not reported	Cooking oil	Methanol (60:1)	1	70	3.5	97.1% yield	Jianxiang W. et al., 2014
Catalysts with sulfonic acid groups Sulfonated Carbon Composite (P-C-SO ₃ H)	The catalyst precursor prepared by drop-wise addition of aq. glucose (1.2 g), glucose, 3 mL deionized water and a small amount H ₂ SO ₄ (~0.2 g) to pre-dried (100°C air) Amberlite XAD1180 to incipient wetness. The mixture was dried at 100–120°C overnight and then pyrolyzed under dry N ₂ at 300°C for 1 h.	BET surface area < 1 m ² /g	Acetic acid	Methanol (2:1)	3	60	1	72.4% conversion	Mo et al., 2008
Sulfated ZrO ₂	ZrOCl ₂ ·8H ₂ O was dissolved in H ₂ O; zirconium hydroxide precipitated at pH = 9 by NH ₃ solution, washed, dried at 120°C for 16 h and impregnated with H ₂ SO ₄ , then calcined at 650°C for 4 h.	SSA = 118 m ² /g	Dodecanoic acid	Methanol (3:1)	3	180	1	96% conversion	Ardizzone et al., 2004
Sulfated zirconia alumina	calcined at 400°C for 2.5 h	Not reported	Sea Mango	Methanol (8:1)	3	180	-	83.8% conversion	Kansedo et al., 2012
Acidic ion exchange resin	The resins were washed with methanol and dried for 12 h	SSA = 53 m ² /g	Waste fatty acid	Methanol (20 vol%)	2	60	1.67	45.7% conversion	Ozbay et al. 2008

Table 2.3 Summary of the activity and reaction conditions of various types of heterogeneous basic catalysts used in biodiesel production

Catalyst	Preparation method	Characterization	Operation parameters					Performance	Refs.
			Feedstock	Type of alcohol (alcohol to oil molar ratio)	Catalyst loading (wt%)	Temperature (°C)	Reaction time (h)		
CaO	CaCO ₃ calcination at 800°C for 3 h	BET surface area = 2.7 m ² /g	Palm oil	Methanol (15:1)	7	60	1	94% conversion	Yoonubek et al., 2010
Sodium titanate nanotubes doped with potassium	10 g of mixed with 150 ml of a 10 M alkali solution, followed by hydrothermal treatment in a Teflon-lined autoclave for 20h upon constant magnetic stirring.	BET surface area = 213 m ² /g	Soybean oil	Methanol (20:1)	1	80	6	99.2% yield	Hernandez Hippolito et al., 2014
Na ₂ PO ₄	Not reported	Not reported	Palm olein	Methanol (18:1)	1	210	0.5	> 95% yield	Khrisaya Porn I. et al., 2014
KOH loaded on ZrO ₂	The catalytic carrier was calcined in at 500°C for 4h and added aqueous K ₂ CO ₃ compound solution slowly then kept for 24 h. After impregnation, the catalysts were calcined at 530 °C for 5 h.	Base strength (pK _{a,H+}) = 9.8-15	S. <i>maritima</i> triglyceride	Methanol (15:1)	6	60	2	86.4% yield	Islam et al., 2015
CaO-based/Au nanoparticles	All powdered samples were then transformed to CaO catalysts using calcination at a different temperature range of 600–900 °C for 4 h and loaded K ₂ CO ₃ for impregnation	Not reported	Heptanoic acid	Methanol (9:1)	3	65	3	90-97% conversion	Bet-Moushouh et al., 2016
Zn,Al-mixed oxides	Zn,Al-catalysts were prepared by coprecipitation, at room temperature, using an aqueous solution of the metallic cations and a highly basic carbonate solution	SSA = 64-161 m ² /g	Soybean oil	Methanol (45:1)	5	182.5	4	86% yield	Vetga et al., 2014
CaO-CeO ₂	CaO were prepared via wet impregnation method and labeled as xCa-Ce, where x = 10- 70 wt.% CaO	BET surface area = 8.6 m ² /g	Palm oil	Methanol (12:1)	5	65	4	95% yield	Wong et al., 2015

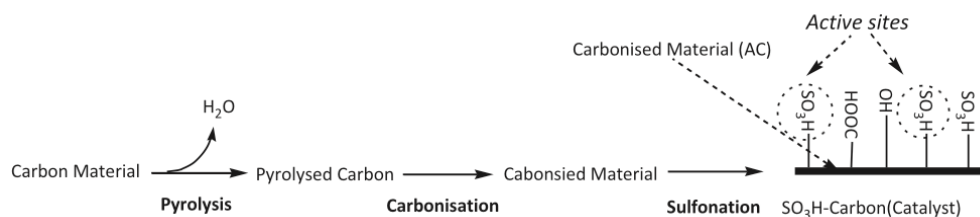


Figure 2.4 Conventional preparation of carbon-based acid catalyst.

Table 2.4 Solid acid catalysts for esterification

Catalysts	Feedstock	Reaction temperature (°C)	Ref
Amberlyst	Soybean oil + oleic acid	80	Park et al., 2010
Amberlyst	Cooking sunflower oil + acid oleic	100	Son et al., 2011
Ionic exchange resin	Soybean oil + oleic acid	100	Tesser et al., 2010
SO_4^{2-}/ZrO_2	Rapeseed oil + miristic acid	120-170	Rattanaphra et al., 2011
WO_3/ZrO_2	Waste acid oil	150	Park et al., 2010
Kaolins	Oleic acid	160	Nascimento et al., 2009
Raw halloysite	Lauric acid	160	Zatta et al., 2011
ZnO/ZrO_2	Brown grease	200	Kim et a., 2011

However, a greener hydrothermal carbonization process has been found by a byproduct of sugar dehydration in hot compressed water (150-250°C). Titirici et al., (2008) used to synthesize carbonaceous materials. In this process, carbonization takes place in water at lower operating temperatures (150-250 °C) under self-generated pressure, thus, drying of the carbon raw materials is not necessary (Titirici et al., 2012). Hydrothermal carbonization is an exothermal process that lowers both the oxygen and hydrogen content of the feed (described by the molecular O/C and H/C ratio) by mainly dehydration and decarboxylation. Many chemical reactions might appear during hydrothermal carbonization have been mentioned throughout the literature such as hydrolysis, dehydration, decarboxylation, condensation polymerization and aromatization. They do not represent consecutive reaction steps but rather form a parallel network of different reaction paths. It is understood that the detailed nature of these mechanisms, as well as their relative significance during the course of reaction, primarily depends on the type of feed (Titirici et al., 2015).

Initially, the formation mechanism of hydrothermal carbon (HTC) was studied employing simple carbohydrates as model system (Titirici et al., 2012). The typical morphologies of hydrothermal carbonization of various mono- and disaccharides and their decomposition product were shown in Figure 2.6. As seen from this figure, very similar morphologies were observed for hexose derived carbon such as glucose and fructose as well as for their composition product HMF (Figure 2.5 a, b, c). Hydrothermal treatment of pentose (e.g. xylose, Figure 2.5 d) as well as of its decomposition product, furfural, while hydrothermal treatment of sucrose, which is a disaccharide consisting of glucose and fructose units, resulted in HTC spheres of various size.

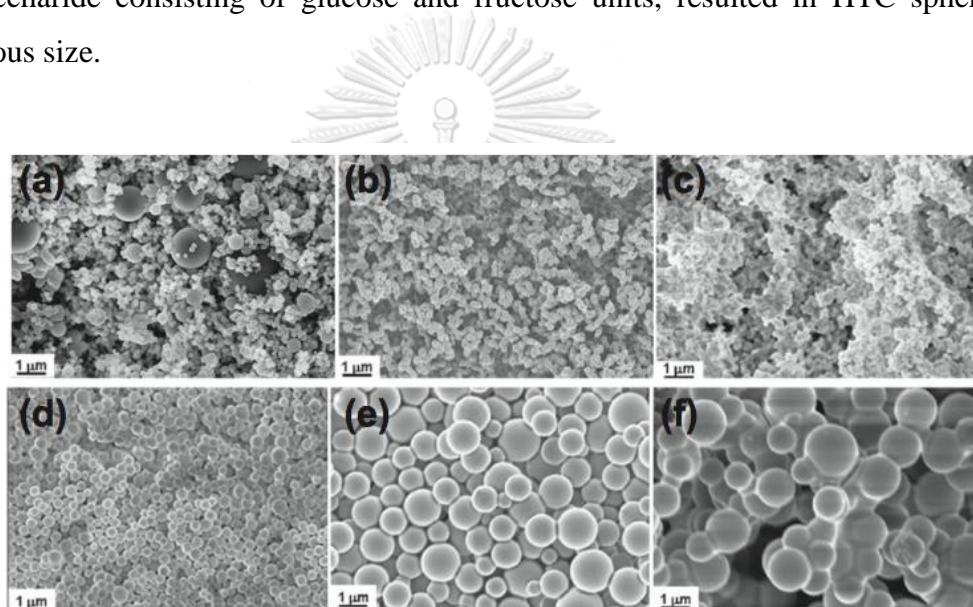


Figure 2.5 SEM micrographs of hydrothermal carbon materials obtained at 180°C from (a) glucose; (b) fructose; (c) hydroxymethylfurfural (HMF); (d) xylose; (e) furfural; (f) Sucrose

Employing the ^{13}C NMR complemented by GC-MS, Titirici (2008) studied the formation mechanism and a final structure of HTC derived from glucose. In their study, HTC was proposed to form upon the dehydration of hexose (glucose and fructose) to hydroxymethylfurfural (HMF) and of pentose to furfural. Once these furans are formed, they then undergo a very complex chemical cascade involving a simultaneous combination of ring-opening reactions to create diketones that can further undergo aldol type condensations with the furan ring, while Diels-Alder reaction may lead to more aromatic features, with concurrent polycondensation

reactions (Figure 2.6). Upon the “polymerization” of HMF or furfural, nucleation takes place followed by growth of the particles upon further incorporation of HMF derived monomers, leading to spherically shaped particles.

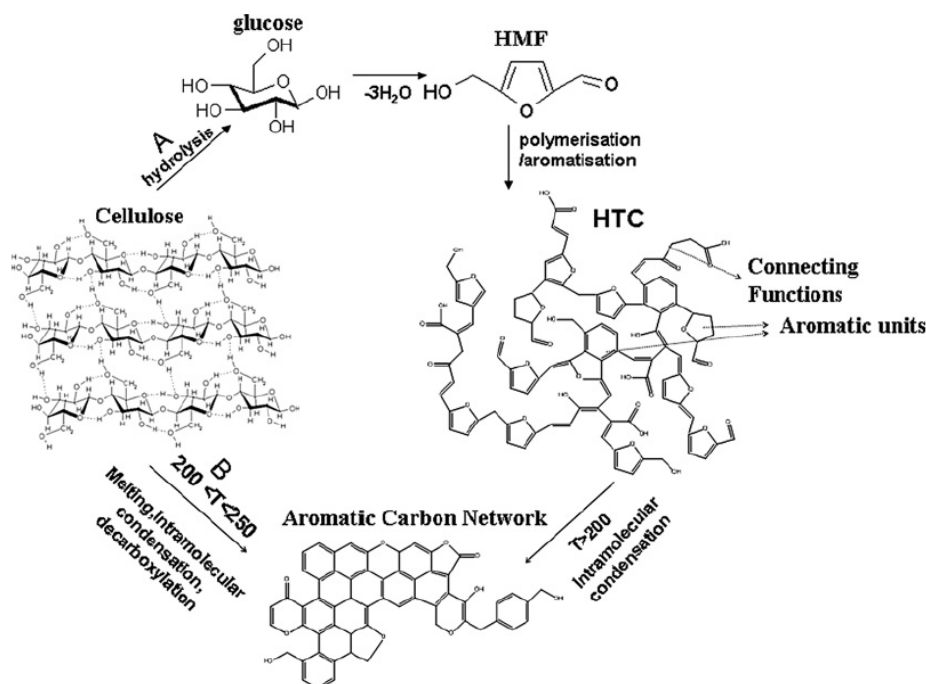


Figure 2.6 Conversion of cellulose into hydrothermal carbon: (A) via HMF resulting in a furan-rich aromatic network; (B) direct aromatization (Baccile et al., 2009).

Moreover, HTC can be activated by increasing the active site of specific functional groups for a particular reaction. The attaching acid functional groups to the hydrothermal carbon using concentrated sulfuric acid, and the resulting material is called sulfonated hydrothermal carbon (sulfonated HTC). Moreover, sulfonated carbons were found from different carbon sources such as single walled carbon nanohorns and carbon microsphere as shown in Table 2.5. These catalysts showed high efficiency of catalytic activity in various reactions with the strong acid of sulfonic groups in spite of the low surface area.

Table 2.5 Sulfonated acid catalysts for esterification

Catalyst	Feedstock	Methanol : oil molar ratio	Reaction temperature (°C)	Reaction time (h)	Performance	Ref.
Sulfonated, carbonized cellulose (0.4 g)	Triolein	3.8:1.7 (wt)	130	5	98.1% yield	Hara et al., 2010
Sulfonated, carbonized D-glucose (0.14 g)	Palmitic, Oleic, Stearic	10:1	80 (reflux)	5	> 95% yield	Marchetti et al., 2008
Sulfonated, carbonized D-glucose (0.5 g)	Waste oil (27.8%FFA)	5.54:5 (wt)	80 (reflux)	15	> 90% yield	
Sulfonated, carbonized D-glucose Impregnated with polymer matrix (AmberliteXAD1180) (3 wt)	Acetic acid	2:1	60	1	72.4 % yield	Mo et al., 2008
Sulfonated-MWCNTs (0.2 wt%)	Cotton seed oil	18:2	240	2	84-85% yield	Shu et al., 2009
Sulfonated, carbonized vegetable oil asphalt (0.2 wt%)	Cotton seed oil	18:2	260	3	89.9% yield	Shu et al., 2010
Sulfonated-carbonized de-oiled canola meal (7.5 wt%)	Canola oil containing high %FFA	60:1	65	24	93.8% yield	Rao et al., 2011
Sulfonated-carbonized lignin (5 wt%)	Jatropha oil containing high %FFAs	12:1	120	5	96.3% yield	Pua et al., 2011
Sulfonated-carbonized corncobs (3 wt%)	Model waste feedstock oil, 12 wt% FFAs	32:1	80	6	98% yield	Arancon et al., 11
Sulfonated-carbonized glycerin (10 wt%)	Triolein	60:1	80	12	25-26% yield	Song et al., 2012
Sulfonated lignin (7 wt%)	Acidified soybean soapstock (56 wt% FFAs)	9:1	70	5	97% (FFA conversion)	Guo et al., 2012

2.1.3 The alternative microwave heating

Microwave (MW) irradiation is the alternative heating source which is internal heating on a molecular basis. There are widely applied in the chemical reactions over the last decade with advantages of an ease of operation, energy transfer instead of heat transfer, heat directly to the selective materials, rapid heat, uniform heating with minimal thermal gradients, short reaction time and energy savings (J.A. Menendez et.al., 2010, Paula M. et al., Wei L. et a., 2013, Lingling M. et. Al., 2016).

MW is electromagnetic energy and belong to the portion of electromagnetic spectrum between 300 and MHz and 300 GHz; a region lies between infrared and radio frequencies as shown in Figure 2.6. MW heating generates rapid superheating due to two main mechanisms of dipolar polarization and ionic conduction. The orientation of dipoles occurs as polar molecules rotates to realign themselves with the rapidly oscillating electric field of the MW (Kostas et al., 2017; Martinez-Guerra et al., 2014; Maso et al.) The reorientation of the molecules results energy loss in the form of thermal energy regarding molecular friction and dielectric loss (Kappe et al., 2012). The unique MW heating is illustrated in Figure 2.7 compared to conventional heating, where MW penetrates the material resulting internal heating and thermal energy is then uniformly dissipated throughout the material.

However, MW heating is based dielectric heating, not all materials can be heated under MW irradiation. Generally, materials divided 3 categories as

- (1) MW transparent/insulator: MW pass through the material without any losses e.g. Teflon, glass, quartz and ceramics.
- (2) MW conduction: MW is reflected by the materials e.g. metals.
- (3) MW absorbing: MW penetrates, absorbed and converted into heat e.g. polar molecules.

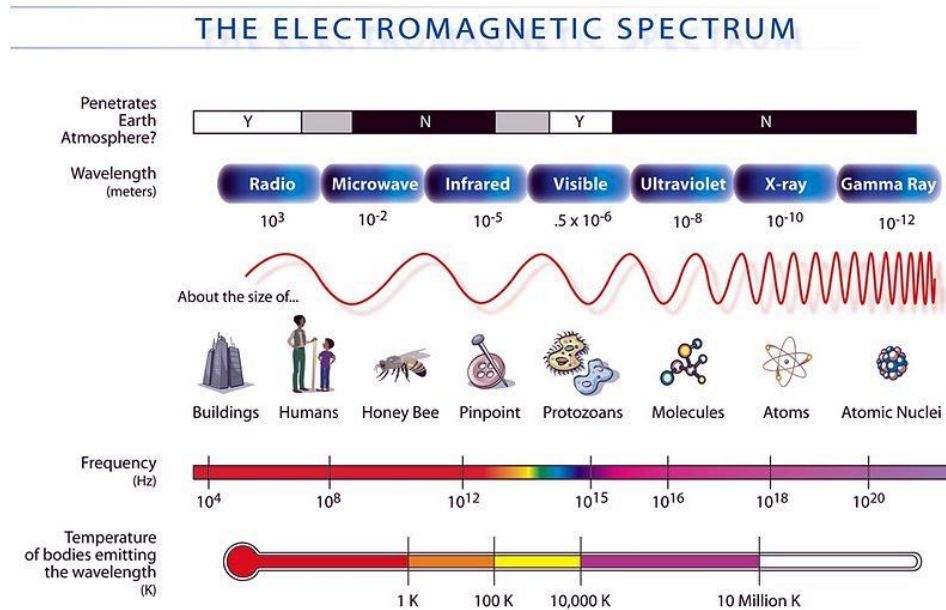


Figure 2.6 The electromagnetic spectrum as a function of frequency

(<https://www.siyavula.com/read/science/grade-10/electromagnetic-radiation/11-electromagnetic-radiation-03>)

The ability of materials to be heated under MW is a very good absorber of MW and can be easily converted MW energy into thermal energy which is defined by dielectric loss tangent. The dielectric loss tangent ($\tan \delta$) equal to the dielectric loss factor (ϵ'') which relates to the dissipation of the stored electrical energy into heat divided by the dielectric constant (ϵ') that determines the capability of the materials for energy storage in the electric field. In the MW field at the frequency 2.45 GHz, the materials as the MW absorber orient and align themselves according to the direction of the electric field with 2.45 billion times per second and heat is generated from the loss of energy through molecules friction. The directly heat of materials on a molecular basis leads to rapid heat and the temperature in-core materials is higher than bulk temperature of the system as called hot spots.

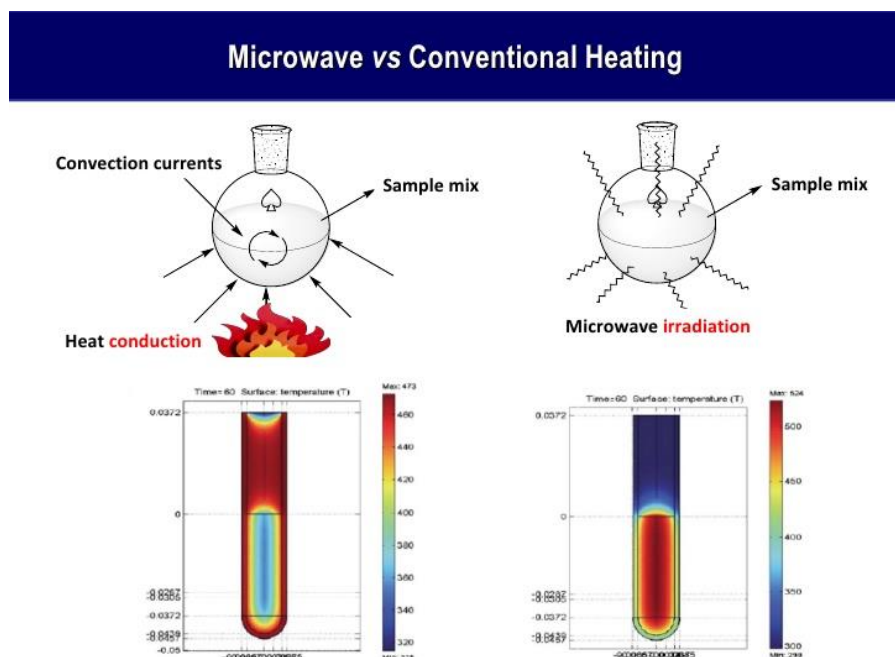


Figure 2.7 The differences in temperature distribution and direction of heat transfer between conventional and MW heating. (<https://wiki.anton-paar.com/en/microwave-assisted-synthesis/>)

The different carbonaceous materials such as activated carbon, graphite, charcoal and carbon nanotube were found to be a good MW absorber (J.A. Menendez et al., 2010). The high capacity of carbon materials to absorb MW energy and convert it into heat is shown in Table 2.6. Therefore, in the case of MW heating, the carbon materials play double role of catalyst and MW absorber contributing to heterogeneous catalytic reactions.

Table 2.6 Dielectric loss tangent of different carbon materials at a frequency of 2.45 GHz and room temperature, ca., 298 K

Carbon material	$\tan \delta = \varepsilon''/\varepsilon'$	Ref.
Coal	0.02-0.08	Yang et al., 1987, Marland et al., 2001
Carbon foam	0.05-0.20	Wu et al., 2008, Challa et al., 1994
Charcoal	0.11-0.29	Atwater et al., 2004, Ma et al., 1997
Carbon black	0.35-0.83	Challa et al., 1994, Atwater et al., 2003
Activated carbon	0.57-0.80	Dawson et al., 2008
Carbon nanotube	0.25-1.14	Lin et al., 2008, Zhang et al., 2009
CSi nanofibres	0.58-1.00	Yao et al., 2008

Microwave accelerated esterification with different heterogeneous catalysts were shown in Table 2.7. In general, the yield of esterification reaction under MW irradiation showed similar results to those obtained from the conventional heating but with very fast heating rates (Melo et al., 2009). An open system and a closed system are used for the reaction under MW irradiation. A microwave program at constant power can be used only with an open system. The maximum temperature can be reached at the boiling point of the solvent, therefore a reflux cooler is needed in this case. While the reaction control of a MW with closed pressure vessels is temperature or pressure sensors. Maximum reaction temperature is depending on thermal stability and pressure rating of the vessels. However, both systems are carried out the biodiesel production due to their advantages of MW heating.



Table 2.7 Esterification of oleic acid with different heterogeneous catalysts under microwave irradiation

Feedstock	Catalyst	MeOH:oil molar ratio	Reaction temperature (°C)	Reaction time (min)	Performance	Note	Ref.
Oleic acid	-	10:1	200	30	51.5% conversion	Synthos 3000-Anton Parr 1400 W	Melo et al., 2009
Oleic acid	Niobium Oxide (5 wt%)	10:1	200	20	68% conversion	Synthos 3000-Anton Parr 1400 W	Melo et al., 2010
Oleic acid	Sulfate Zirconia (5 wt%)	20:1	60	20	90% conversion	MW heating system with reflux	Kim et al., 2011
Oleic acid	Amberlyst 15 dry (10 wt%)	20:1	60	15	66.1% conversion	MW heating system with reflux	Kim et al., 2011
Oleic acid	Bi(OTf) ₃ (1% mol)	48:1	150	1	88% conversion	Biotage MW reactor	Socha et al., 2010
FFA stearic	D418	11:1 (EtOH)	80	7 h	>90% conversion	Power not available	Liu et al., 2013
Linoleic	Sc(OTf) ₃ (1% mol)	48:1	150	1	97% conversion	Biotage MW reactor	Socha et al., 2010
Palmitic	Bi(OTf) ₃ (1% mol)	48:1	150	1	99% conversion	Biotage MW reactor	Socha et al., 2010
FFA Palm oil	Dowex 50X2 (10% wt oil)	20:1	60	60	95.6% conversion	Domestic MW 1000 W	Mazo et al., 2010
FFA Palm oil	Amberlite IR120 (10% wt oil)	20:1	60	60	91.3% conversion	Domestic MW 1000 W	Mazo et al., 2010
FFA Palm oil	Amberlyst 15 (10% wt oil)	20:1	60	60	91.4% conversion	Domestic MW 1000 W	Mazo et al., 2010

2.2 Design of experiment

Traditionally, unknown effects or parameters are usually carried out under controlled conditions to test a hypothesis. Then, experiment results are analyzed to evaluate a significant impact on the process. It is monitored only one parameter changing with constant other parameters (called one-variable-at-a-time or one-factor optimization). It does not show the interactive effect among parameters studies which is the major disadvantage of this method. Design of experiments (DoE) or experimental design is a tool used in analytical optimization to overcome the problem above. It can also be evaluated inputs effects on the process output, and can be predicted inputs should be to achieve a desire output.

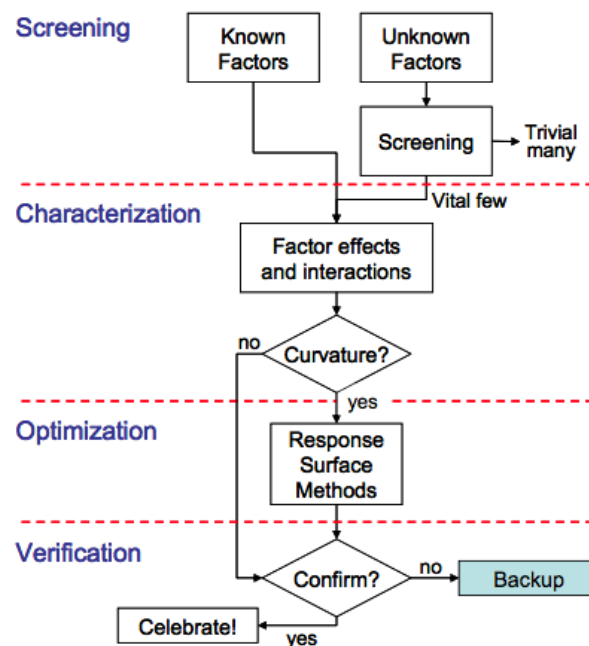


Figure 2.8 Design of experiment sequences (Shari Kraber, Stat-Ease, Inc., Minneapolis, MN)

DoE can be divided into 4 main parts: screening, characterization, optimization and verification as shown in Figure 2.8. Screening studies is the selection of independent factors effecting on the process. Next, factor effect and its interaction are investigated by characterization. Response surface methodology (RSM) is a one technique of optimization by collecting mathematical and statistical

information based on the fit of polynomial equation to the experimental data. Lastly, the verification is necessary to confirm validation of optimization. The advantages of DoE are reducing design costs by minimizing process variation and decreasing rework as well.

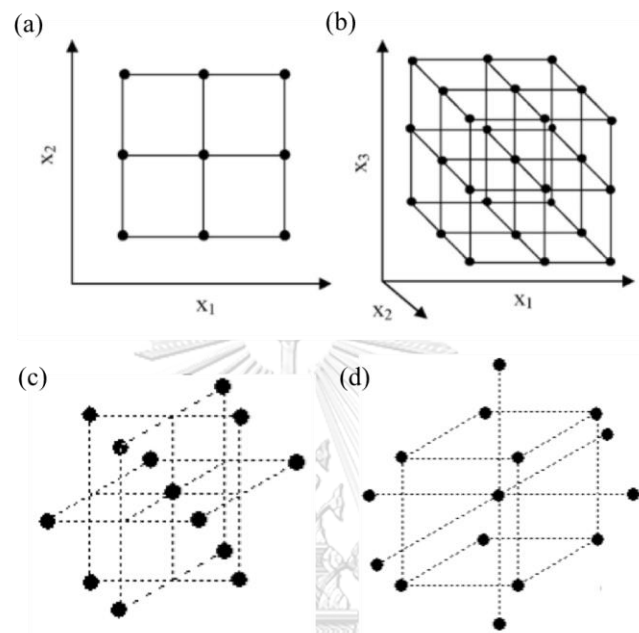


Figure 2.9 Experimental design based on studies factors in three levels for the optimization of (a) two factors (b) three factors and three factors experimental design type (c) Box-Behnken design (d) Central Composite design

The fundamental experimental design relates to randomization, replication, and factorial experimentation. Randomization is a method to eliminate potential biases distorting the results of the experiment. While, a replicate is a complete repetition of the same experimental conditions for increasing the precision output. Factorial or multi-factor design is a method to understand the influent of each factor and the combinations of factors. A full three-level factorial design (FFD) requires 3^k (k is a number of studied factors) experimental runs as shown in Figure 2.9 (a,b).

In practical, smaller number of experimental points is present when the factor number is higher than 2 such as the Box-Behnken and central composite design Box-Behnken design (BBD) is defined by a “wire frame” with the edges inside the box

(Figure 2.9 (c)). The number of experiment requires for BBD is $2k(k-1)$ and a center point. It based on three levels as -1, 0 and +1 as shown in Table 2.4. BBD with two factors does not exist (it is FFD with 9 points), the three factor has default on this design. The advantage of the BBD is more economical compare to FFD due to lower experimental runs (Table 2.8). Table 2.5 shows BBD applications in analytical chemistry. However, its applications it still lower in comparison with CCD (Bezerra et al., 2008).

Table 2.4 Box-Behnken experiment matrices design at three level for two factors (a) and three factor (b)

(a)		(b)		
X_1	X_2	X_1	X_2	X_3
-1	-1	-1	-1	0
-1	0	1	-1	0
-1	1	-1	1	0
0	-1	1	1	0
0	0	-1	0	-1
0	1	1	0	-1
1	-1	-1	0	1
1	0	1	0	1
1	1	0	-1	-1
		0	1	-1
		0	-1	1
		0	1	1
		0	0	0

Table 2.5 Applications of Box–Behnken design.

Analytes	Samples	Objectives	Ref.
Aliphatic aldehydes	Potato crisps	Optimizing the conditions for the [32] derivatization reaction of the analytes with 2,4-dinitrophenylhydrazine	Stafiej et al., 2006
Cadmium	Drinking water	Optimizing an on-line pre-concentration system [34] using knotted reactor	Souza et al., 2005
Neuropeptides	Biological	Optimizing the main electrophoretic parameters [36] involved in the analytes separation	Babu et al., 2004
Lead	Waters	Optimizing a flow injection system for the on-line [37] pre-concentration of these metal using silica gel functionalized with methylthiosalicylate	Zougagh et al., 2004
Sulphonamides, dihydrofolate reductase inhibitors and beta-lactam antibiotics	Food products	Optimizing the simultaneous separation of these [40] substances	Hows et al., 1997

Central composite design (CCD) was presented by Box and Wilson (also known as Box-Wilson design). This design consists of three types of points: factorial points, axial or star points and center points. A graphic of a three-dimensional CCD is shown in Figure 2.10. All factors are studied in five levels as $-\alpha$, -1 , 0 , 1 , α resulting the requirement experiment number is $2^k + 2k$ and replicate center points (Table 2.6, 2.8). It is efficient to estimate full second-order model such as main effects, two-way interaction and quadratic effects. Some applications of CCD are shown in Table 2.7.

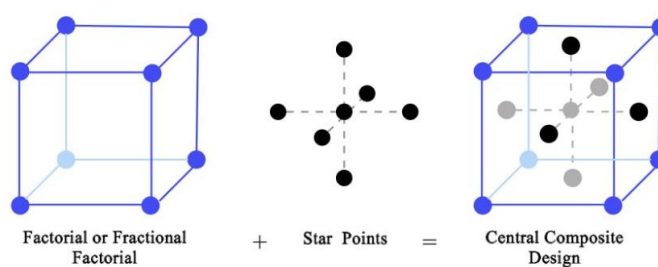
**Figure 2.10** Construction of CCD

Table 2.6 Central composite experiment matrices design at three level for two factors (a) and three factor (b)

(a)			(b)			
	X_1	X_2		X_1	X_2	X_3
Factorial	-1	-1	Factorial	-1	-1	-1
	1	-1		1	-1	-1
	-1	1		-1	1	-1
	1	1		1	1	-1
Axial	$-\alpha$	0	Axial	-1	-1	1
	α	0		1	-1	1
	0	$-\alpha$		-1	1	1
	0	α		1	1	1
Center	0	0	Center	$-\alpha$	0	0
				α	0	0
				0	$-\alpha$	0
				0	α	0
				0	0	$-\alpha$
				0	0	α
				0	0	0

Table 2.7 Applications of Central composite design.

Analytes	Samples	Objectives	Ref.
Nickel	Petroleum	Developing a procedure for the direct determination of Ni using a solid sampling strategy	Brandão et al., 2006
Mercury	Gasoline	Optimizing a method for direct aqueous NaBH_4 reduction of metal in microemulsion medium	Lo'pez et al., 2007
Volatile compounds	Vinegar	Optimizing the extraction and desorption analytical conditions of a stir bar sorptive extraction for these analytes	Guerrero et al., 2006
Chlorobenzenes	Environmental water	Developing a headspace single-drop micro-extraction procedure using room temperature ionic liquid for determination of trace amounts of these substances	Vidal et al., 2007
Aluminum	Juices and soft drink	Developing a preparation method based on ultrasound-assisted pseudo-digestion	Jalbani et al., 2006

Table 2.8 The requirement number of experiments of FFD, BBD and CCD.

Design		k = 2	k = 3	k = 4	k = 5
FFD	3^k	9	27	81	243
BBD	$2k(k-1) + \text{Center point}$		13	25	41
CCD	Factorial points; 2^k	4	8	16	32
	Axial or star points; $2k$	4	6	8	10
	Center points	5	5	6	6
	Total	13	19	30	48

The response variables (output) are determined in polynomial equation (Taylor series) once screening experiments and the important factors has been performed to produce a prediction model, to determine curvature, to detect interactions among factors and to optimize the process. The response variables; Y as a function of the input variables; X as shown in Equation (1).

$$Y = \beta_0 + \sum_{i=1}^p \beta_i X_i + \sum_{i=1}^p \sum_{j=1}^p \beta_{ij} X_i X_j + \sum_{i=1}^p \sum_{j=1}^p \sum_{k=1}^p \beta_{ijk} X_i X_j X_k + \dots,$$

where

β_0 = the overall mean response

β_i = the main effect for factor ($i=1, 2, \dots, p$)

β_{ij} = the two-way interaction between the i th and j th factors

β_{ijk} = the three-way interaction between the i th and j th, and k th factors

The X represents each factor, denoted by +1 and -1 as a code of high and low range of control factor, respectively. Interaction between factors show the effect of the response factor to another factor. A mathematical model relates to the response variables with the factor effects which need to consider the following criteria to a good fit model to the experimental data (Granato et al., 2014):

- Standard deviation of the factors and model
- Statistical significance of factors

- Regression coefficient (R^2)
- Significance of the regression

Analysis of variance (ANOVA) was employed to statistically assess the adequacy of each factor for the response. Fisher F -test in the form of F -value indicates the fitness of the experimental model. While, the significance model in fitting of the experimental data is within the confidence level of 95% (P -value less than or equal 0.05). It means the smallest P -value is defined as the most significant factor in the process. Lastly, regression coefficient (R^2) evaluates the quality of model fitting. Moreover, response surface plots are used to visualize the interactions of factors on the responses.

Recently, RSM based on CCD has been reported in many literatures to optimize esterification reactions in various catalysts (Trinh et al., 2018, Peng-Lim et al., 2013, Hasni et al., 2017, Ma et al., 2015). From the literature reviews, the main parameters affecting the reaction are reaction temperature, reaction time, molar ratio of oil to alcohol, and catalyst loading.

2.3 Kinetic study

The main goal of chemical kinetics is to investigate the mechanism of a chemical reaction and to predict the rate of reaction. Moreover, the understanding of chemical kinetics is very important to select suitable reaction system and most efficient operation at a commercial scale. At present, heterogeneous catalysts play a significant role in chemical process. The rate in the catalytic mechanism is necessary to design of new and more effective of catalyst. Therefore, kinetic studies aim to identify reaction mechanism and to study how rates are affected by the reaction conditions and the catalyst properties (Francoise et al., 2014). In recent year, the esterification reactions were proposed for homogeneous and heterogeneous systems as shown in Table 2.9. The lower value of the activation energy value refers to the efficiency of the catalyst and it is important in analyzing the reactive process to evaluate the potential of the catalyst in industrial application.

Table 2.9 Summary of kinetic studies on esterification reaction of oleic acid.

Catalysts	Alcohol to oil ratio	Temperature ranges (°C)	Time ranges (hrs)	Kinetic parameters		Heating source	Ref.
				Order	E_a (kJ/mol)		
Amberlyst 15	EtOH (1:2)	40-70	0-3 h		113.87	Conventional with reflux	Ahmedzeki et al., 2013
H ₂ SO ₄	EtOH (1:6)	40-70	0-3 h		26.63	Conventional with reflux	Abbas et al., 2013
zinc acetate	MeOH (1:4)	160-220	0.1	2.2	32.62	Supercritical	Song et al., 2010
H ₂ SO ₄	MeOH	30-70	0-1.2		32.62	Ultrasonic	Supranukmi et al., 2015
Sulfated cation exchange resin	EtOH (1:9)	40-82	1-8	pseudo-homogeneous	24.8	Conventional with reflux	Jiang et al., 2013
Cation exchange resin/polyethersulfone hybrid catalytic membrane		50-240	0-8	pseudo-homogeneous	73.75	Conventional with reflux	Zhang et al., 2012
NaY Zeolite catalyst	EtOH (1:6)	40-70	0-2.5		42.69	Conventional with reflux	Abbas et al., 2013
Magnetic ionic liquid	MeOH (1:22)	40-70	0.5-3.6	pseudo-first order	17.97	Conventional with reflux	Fauzi et al., 2014
Aminophosphonic acid resin, D418	EtOH (1:11)	60-80	0-12		55	Microwave	Liu et al., 2013
H ₂ SO ₄	MeOH (1:10)	50-70	0-0.5	2	53.72	Microwave	Lieu et al., 2016

CHAPTER III

MATERIALS AND METHODS

3.1 Materials and chemicals

The carbon precursor, D-glucose and sulfuric acid (laboratory grade, 98%) were purchased from Fluka, Singapore. Methanol (laboratory grade, 99% purity) was purchased from Wako, Japan. Oleic acid (OA) and n-hexane were purchased from Sigma-Aldrich, United States. The reference methyl oleate standard and internal standard, 2,6-Dimethylnaphthalene (DMN) were purchased from GL Science Inc., Japan and Sigma-Aldrich, United States, respectively.

3.2 Preparation and characterization of hydrothermal carbon-based acid catalyst (S-HTC)

3.2.1 Hydrothermal carbon (HTC) preparation

The hydrothermal carbonization process was performed in 600 ml high pressure reactor (Parr, USA, Figure 3.1) filled with 30 g of glucose and 300 ml of deionized water. The reactor was then heated at 220°C for 6 hours under nitrogen atmosphere. The resulted HTC was washed with distilled water until no pH change was observed in the filtrate and the retentate was dried at 110°C overnight.

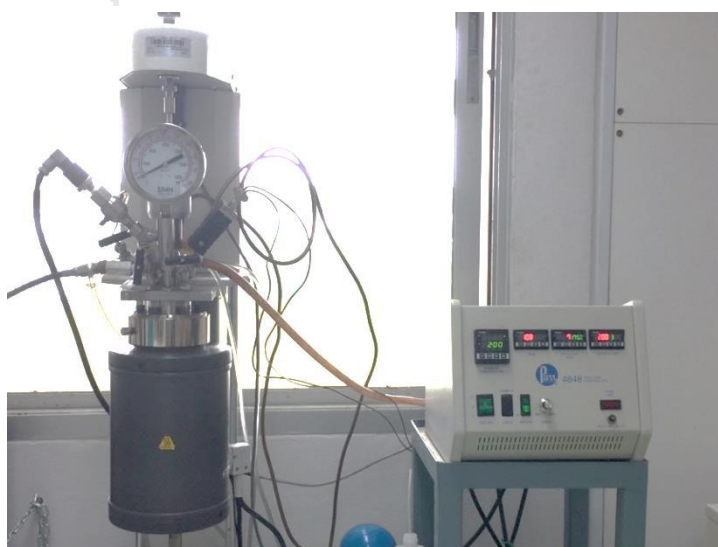


Figure 3.1 Parr reactor for hydrothermal carbonization

3.2.2 Acid functionalized hydrothermal carbon preparation

A sulfonic acid groups were introduced into the HTC by heating 10 g of HTC in 100 ml of concentrated sulfuric acid in the 3-neck round bottom flask at 150°C for 15 hours under nitrogen flow. A 1-liter flask containing activated carbon was connected to the reaction flask to adsorb the acid vapor. The nitrogen inlet flow was switched off when the reaction reached the desired reaction time. The set-up experiment for acid functionalization was shown in Figure 3.2. After cooling, 1 liter of distilled water was added to the mixture and filtered. The black solid was then repeatedly washed with hot distilled water until no sulfate ions were detected. The S-HTC catalysts were then dried in oven at 110°C overnight.



Figure 3.2 The set-up experiment for sulfonation

The synthesized S-HTC were confirmed the physical and chemical characterization by elemental (C, H, N, S), BET, FTIR, TGA, XRD, SEM and acidity analyses in comparison with HTC.

Elemental analysis

The components of catalyst before and after hydrothermal carbonization were determined by CHNS elemental analyzer (LECO CHNS-932, VTF-900) at STREC, Chulalongkorn University, Thailand.

BET surface area

The specific surface area of all catalysts was determined by N₂ physisorption technique using a BELSORP mini-II by BET method. Solid catalysts were analyzed for the BET surface area using a Belsorp-max TPD pro (BEL Japan, Tokyo, Japan) with thermal conductivity detector (Semi-diffusion type, 4-element W-Re filament) at the National Nanotechnology Center, Thailand.

Fourier transform infrared spectroscopy (FT-IR)

Identification of functional groups was analyzed by FT-IR (Perkin-Elmer, Spectrum One) at STREC, Chulalongkorn University, Thailand. All catalysts were characterized the functional groups before and after acid functionalization.

Thermogravimetric analysis (TGA)

The thermal analysis is a method in which changes in physical and chemical properties of materials are measured as a function of increasing temperature (with constant heating rate), or as a function of time (with constant temperature and/or constant mass loss) using Perkin Elmer, TGA 7 (Massachusetts, USA) at STREC, Chulalongkorn University, Thailand. The temperature was raised up to 1000 °C under nitrogen, at a constant rate of 10 °C/min. The thermal decomposition of both hydrothermal carbon-based acid catalysts and one step carbonization and acid functional catalysts were analyzed for stability of the catalysts.

Scanning electron microscope (SEM)

The morphology of before and after of hydrothermal carbon-based acid catalysts and one step carbonization and acid functional catalysts were examined by SEM (JEOL, JSM 6400, Tokyo, Japan) at STREC, Chulalongkorn University, Thailand.

Titration method

The total acid property of carbon-based acid catalysts was analyzed by titration method to determine the Brønsted acid sites on the surface of the catalysts . Sodium hydroxide)0.01 M, 20 ml (solution was mixed with the catalyst)0.04 g(, under constant stirring at room temperature for 2 hours .Then, the resulted filtrate was titrated by hydrochloric acid)0.001M (after separation from the mixture.

3.3 Esterification of OA with methanol

3.3.1 Catalytic activity

Firstly, the isolation parameters of S-HTC, MW and hexane affecting the esterification was studied compared with the conventional heating as a control experiment. The reaction was carried in the absence of S-HTC at reaction temperature of 100°C, reaction time of 60 min, 1:10 molar ratio of OA to methanol under MW heating compared to conventional heating (The 8.8 ml stainless steel reactor, AKICO, Japan (Figure 3.3)).

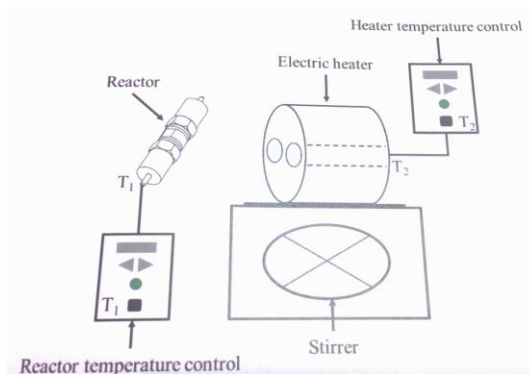


Figure 3.3 Stainless steel reactor, AKICO, Japan

To study the synergy of S-HTC and MW effect, the reactions were carried out by adding 5 wt% S-HTC catalyst under microwave irradiation (Microwave Accelerated Reaction System, MARS6, CEM, USA) as shown in Figure 3.4. There are 12 microwave transparent vessels with microwave power output of 0-1200 W at a frequency of 2.45 GHz. The temperature in the control vessel was monitored by thermocouple and that of the other vessels by infrared sensor. When the temperature reached to the desire temperature, the microwave power is automatically cut off to maintain the constant temperature. When sulfonated HTC and hexane under MW were combined, the reactions were carried out at 5 wt% S-HTC catalyst and Hexane/Methanol = 1.8 (v/v).

Secondly, the reaction was carried out using microwave irradiation to study a single variable study under the following conditions: reaction temperature (50,75,100 °C), reaction time (30, 45, 60 min), molar ratio of OA to methanol (1:1, 1:10, 1:25, 1:40), catalyst loading (0, 1, 2.5, 5, 10wt%) and amount of hexane to methanol ratio (H/M= 0, 0.5, 1, 1.5, 2 (v/v)).

After the reaction, the system was cooled down automatically. The reaction products were discharged from the vessel and were allowed to settle into two phases. The top phase consisted of OAME and unreacted methanol, while the bottom phase is by product of water. Unreacted methanol was removed by evaporator, then OAME was drawn for the quantitative analysis by gas chromatography (GC-FID, Shimadzu, Japan) equipped with a flame ionization detector (FID) and a 5MS capillary column (0.25 μm x 0.25 mm x 30 m, Agilent Technologies, Inc., Japan). The helium was used as a carrier gas. The temperatures of the injector and the detector were kept at 270°C and 310°C, respectively. A 20 μl of OAME sample was dissolved in 180 μl of n-hexane using DMN as an internal standard. The OA conversion was calculated using following equation:

$$\% \text{ Conversion} = \frac{\text{mol of OAME}}{\text{mol of OA}} \times 100 \quad (1)$$

where OAME represents the quantification by GC-FID of OAME.

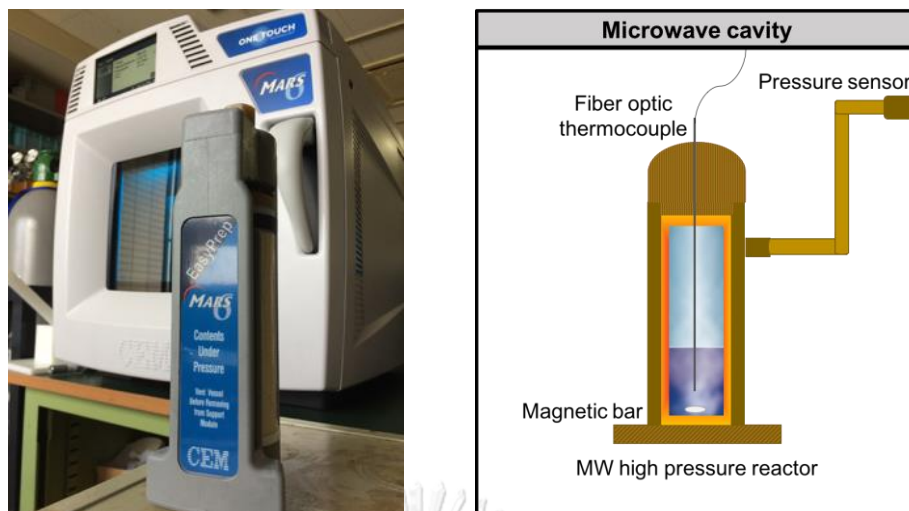


Figure 3.4 Microwave reactor, MARS6 (CEM) and Easy Prep: high pressure vessel

3.3.2 Optimization study

3.3.2.1 Screening parameters effect

In order to optimize condition on esterification, the screening parameters is needed to select the independent factors effecting on the process. The influence of three parameters namely, molar ratio of methanol to OA (1:1, 1:5, 1:10, 1:20), reaction time (15, 30, 45, 60 min) and catalyst loading (0, 1, 2.5, 5, 10 wt%) were studied at fixed reaction temperature of 100°C under MW irradiation. The other parameters were fixed at the lowest condition to study the main parameter. For molar ratio of methanol to OA at 1:1, 1:5, 1:10, and 1:20 were conducted at reaction time of 15 min and 1 wt% catalyst loading. The reaction time effect of 15, 30, 45 and 60 min were studied at 1:1 molar ratio of methanol to OA and 1 wt% catalyst loading. Lastly, the catalyst loading of 0, 1, 2.5, 5 and 10 wt% were evaluated at 1:1 molar ratio of methanol to OA for 15 min.

3.3.2.2 Design of experiment, analysis and model fitting

In this work, parametric optimization of esterification condition was conducted by using Response surface methodology (RSM) with a central composite design (CCD) to evaluate the effect of each parameter and interaction of parameters via quadratic model. Experimental results showed the parameter(s) significantly

affected the OA conversion by statistical tool, the analysis of variance (ANOVA). The suggested optimum condition was confirmed validation through the experiments and to prove the effectiveness of the model.

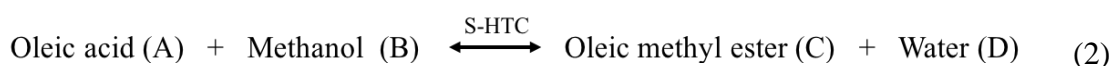
The experiment of S-HTC catalyzed esterification was designed using RSM provided by Expert Design version 10 (Stat-Ease Inc. (2016), USA). A set of experiments was carried out at a fixed temperature (100°C) using pulsed MW to determine the influence of three parameters, namely, molar ratio of methanol to OA (A), reaction time (B) and catalyst loading (C) and their interactions. Using CCD at 3 levels: low, middle and high, designated as -1, 0 and +1 respectively, as shown in Table 1, 17 experimental runs: 8 factorial points, 6 axial points and 3 replicates at the center point, were carried out. A quadratic model using regression analysis was fitted to the values of OA conversion using both linear and non-linear forms. The conformity between experimental and predicted response of the model and the significance of the operating variables were evaluated based on the analysis of variance (ANOVA) and the regression coefficient (R^2).

Table 3.1. Levels of actual and coded factors

Factors	-1	0	1
Molar ratio of methanol to oil (mol)	2.5	5	7.5
Reaction time (min)	50	60	70
Catalyst loading (wt %)	1.5	2.5	3.5

3.3.3 Kinetics study of S-HTC catalyzed esterification

Esterification of OA with methanol, under the catalysis of S-HTC, produces OAME and water as shown by equation (2). The rate of reaction strongly depends on temperature, thus the operating temperature was varied out in the range of 70-100°C under the optimized condition previously determined; methanol to OA molar ratio of 5.831:1 and 3.047 wt% catalyst loading for 0, 15, 30, 45 and 60 min.



A kinetic model was set up on the basis that the influence of the reverse reaction was negligible, due to the excess amount of methanol used. Regarding the Le Chatelier's principle, changing the concentration of a chemical will shift the equilibrium to the minimum concentration side. The reaction rate equation was simplified to the first order pseudo-homogeneous equation.

$$-r = -\frac{dC_A}{dt} = kC_A \quad (3)$$

where C_A denotes the concentration of OA and k is forward reaction rate constant.

For a constant volume system, an OA conversion; X_A is a convenient term used in place of concentration of OA, C_A , and is expressed as in the following equation.

$$C_A = \frac{N_A}{V} = \frac{N_{AO}(1-X_A)}{V} = C_{AO}(1-X_A) \quad (4)$$

where N_{AO} and N_A are the initial mole amount and mole amount of OA, respectively. C_{AO} represents the initial concentration of OA and V is the constant volume.

Hence, equation (3) becomes

$$-\frac{dC_A}{dt} = kC_{AO}(1-X_A) \quad (5)$$

The integrals of Eq. (5) was calculated from

$$-\ln(1-X_A) = kt \quad (6)$$

Thus, the rate constant, k , can be obtained by a linear fit of equation (6). The activation energy can be calculated from the relation of rate constants at different temperatures by the Arrhenius equation.

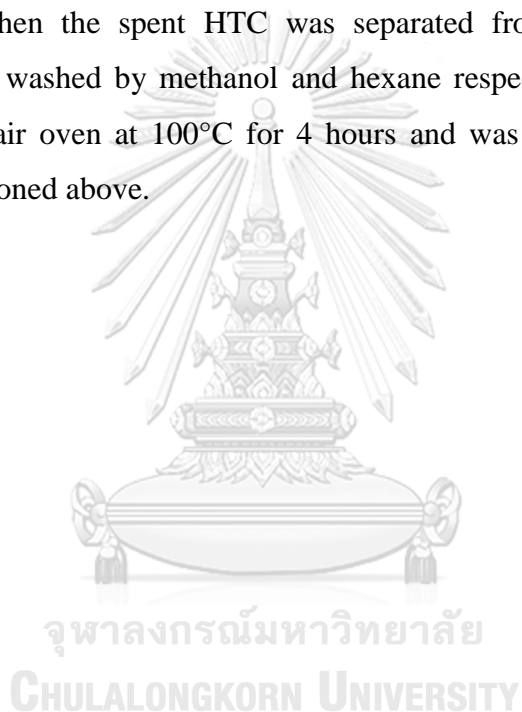
$$k = Ae^{-\frac{E_a}{RT}} \quad (7)$$

where A is the frequency factor and E_a is the activation energy. After linearization, equation (7) becomes:

$$\ln k = -\frac{E_a}{RT} + \ln A \quad (8)$$

3.3.4 Reusability of S-HTC on esterification

The stability of sulfonic groups was tested in catalyst reuse. After fresh catalyst was evaluated in MW assisted esterification reaction of OA and methanol under the optimum condition at methanol to OA molar ratio = 5.831:1, 3.047 wt% catalyst loading then the spent HTC was separated from the product by paper filtration and was washed by methanol and hexane respectively. The spent S-HTC was dried in hot air oven at 100°C for 4 hours and was reused again at the same condition as mentioned above.



CHAPTER IV

RESULTS AND DISSCUSSION

This chapter is the results and discussion of OA conversion to obtain OAMEs using sulfonated hydrothermal carbon-based acid (S-HTC) as catalyst. Firstly, the catalytic activity of S-HTC was test in preliminary experiments. The screening parameters were conducted to find the range of independent parameters for experimental design. Then, the parametric optimization was determined by using Response surface methodology (RSM) with a central composite design (CCD). Moreover, the kinetics study was performed to determine the kinetic parameters important for future process design. Lastly, the reusability of S-HTC was also studies the catalyst stability.

4.1. S-HTC characterization

The physicochemical characteristics of the HTC and the S-HTC catalyst are summarized in Table 4.1 and Figure 4.1-4.4. From the elemental analysis results in Table 4.1, it is noted that the HTC derived from glucose had relatively high oxygen content (O/C ratio = 0.42). The increase in the oxygen content from the O/C ratio = 0.42 to the O/C ratio=0.79 after sulfonation, indicated that sulfonic acid group (-SO₃H) was successfully attached to the HTC by the process.

Table 4.1. Physiochemical properties of HTC and S-HTC.

Sample	Elemental compositions				Atomic ratios		Surface area** (m ² /g)	Total acidity (mmol/g)
	%C	%H	%O*	%S	H/C	O/C		
HTC	66.31	5.96	27.73	N.D.	0.09	0.42	2.90	0.62
S-HTC	53.13	3.42	42.09	1.36	0.06	0.79	2.67	4.90

N.D. Not detected

*The oxygen composition was calculated by difference from 100% considering the other elements.

**BET surface area estimated from N₂ adsorption results

The functionalization of sulfonic acid groups onto the prepared HTC was also verified by the sulfur content of the S-HTC, which was determined to be 1.36% on a mass basis by the elemental analysis. In addition, an increase in the total acidity, determined by titration method, was also observed for S-HTC. This value included both the weak acid ($-\text{COOH}$) and the strong acid ($-\text{SO}_3\text{H}$). Despite the high acid density, the specific surface areas of both HTC and S-HTC were relatively low ($<3 \text{ m}^2/\text{g}$), probably due to low temperature of the hydrothermal carbonization process. Slightly lower specific surface area of S-HTC than that of HTC was probably resulted from the particle agglomeration, as observed from the SEM image shown in Figure 3.1. The morphological structures of the HTC and S-HTC were observed under a scanning electron microscope (SEM). The glucose derived HTC particles have a typical spherical shape with the approximate size of $0.5 \mu\text{m}$, which tend to agglomerate into large particles. The S-HTC was found to have similar morphology but with rougher surfaces.

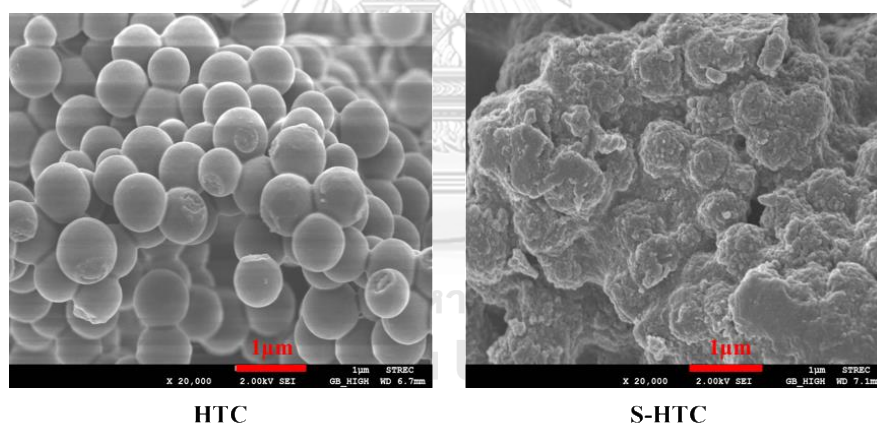


Figure 4.1 SEM Images of HTC before (a) and after sulfonation (b)

The FT-IR spectra in Figure 3.2 confirmed the existence of sulfonic acid functional groups, $\text{O}=\text{S}=\text{O}$ symmetric stretching at 1020 cm^{-1} and $-\text{SO}_3\text{H}$ at 1167 cm^{-1} after sulfonation of the HTC. Also, the absorbance at 1704 cm^{-1} exhibited the presence of carboxylic acid groups. This result suggested that at least two types of Brønsted acid sites: sulfonic and carboxylic acid sites, were present in the prepared S-HTC, which are common acid sites found in carbon-based solid acid catalysts (Valle-Vigón et al., 2012; Pileidis et al., 2014; Tran et al., 2016). The XRD profiles of the

HTC and S-HTC are shown in Figure 1 (c). The broad C diffraction peaks ($2\theta=10^\circ$ - 30°) suggested the amorphous structures of the samples (Malins et al., 2015).

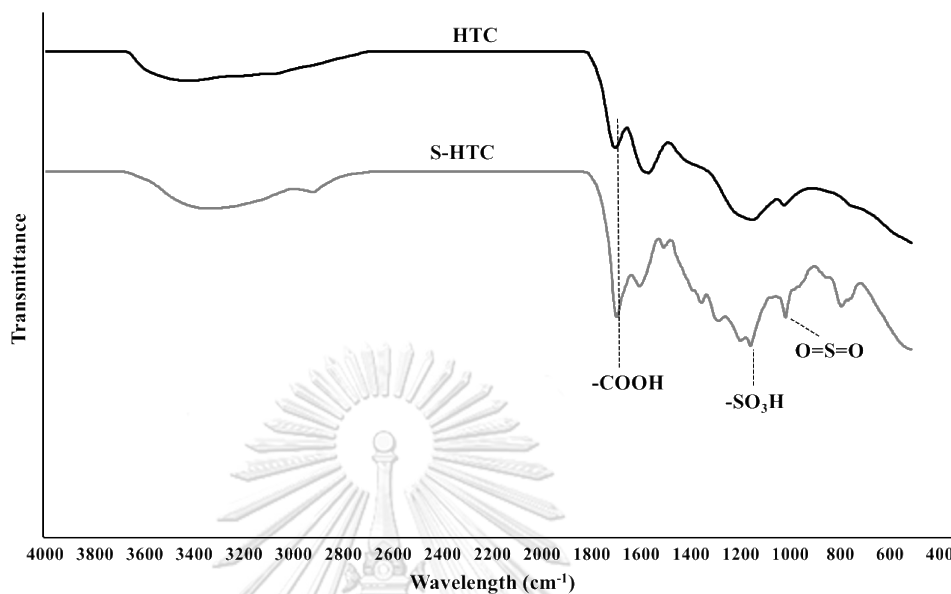


Figure 4.2 FTIR spectrum of HTC before (a) and after sulfonation (b)

The thermal stability of the sulfonic groups attached to the prepared HTC, HTC before and after sulfonation were tested and the results of the TGA analyses are shown in Figure 1 (d). From the TGA profile, HTC showed about 5% weight loss at around 250°C , which corresponded to the loss of some functional groups (-OH mainly and some -COOH) (Pileidis et al., 2014). While the S-HTC showed similar trend with slightly higher weight loss. It can be described by these results that the -SO₃H groups on the surface of the HTC might be stable at a temperature as high as 250°C regardless of some weight loss, before they started to deactivate from the carbon structure (Liu et al., 2013).

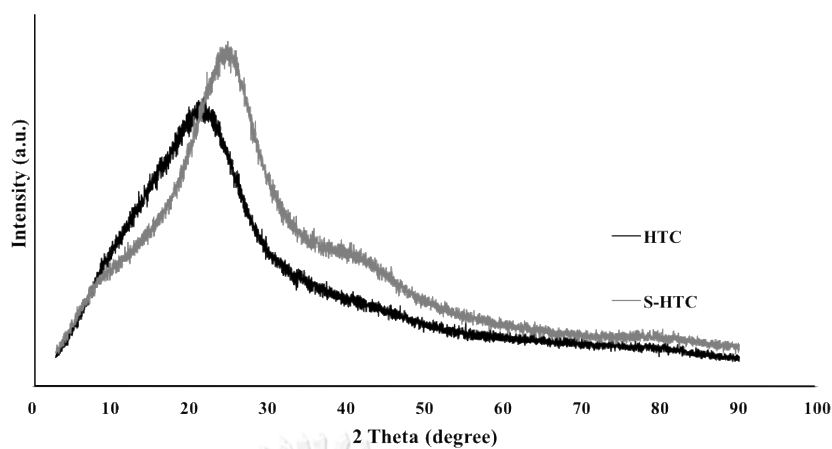


Figure 4.3 XRD of HTC before (a) and after sulfonation (b)

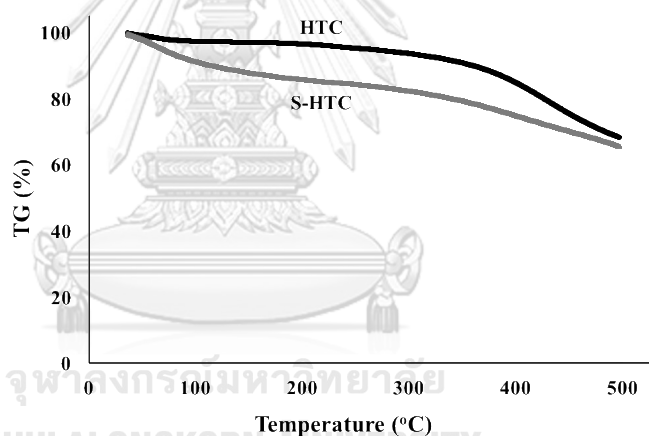
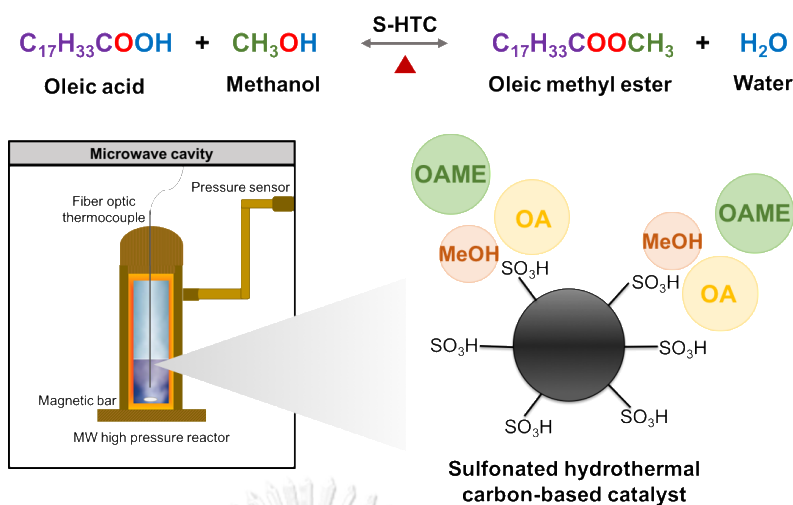


Figure 4.4 TGA of HTC before (a) and after sulfonation (b)

4.2. Catalytic activity of S-HTC on esterification reaction

4.2.1 Screening parameters effect

The catalytic activities of S-HTC were evaluated for esterification of OA with methanol under MW as shown in Scheme 4.1. During the reaction, a magnetic stirring bar was put inside the microwave reactor to attain completely homogeneous mixture of reactants at constant rate. Oleic acid reacts with methanol utilizing the surface functionalities of the catalyst to produce oleic methyl ester (OAMEs).



Scheme 4.1. Schematic diagram showing the esterification reaction takes place at the surface of S-HTC catalyst under MW irradiation

Firstly, in order to isolate the parameters (S-HTC, MW and hexane) affecting the esterification reaction, the experiments were conducted using OA and methanol with molar ratio of 1:10 at 100°C for 60 min under conventional heating as a control experiment (Figure 4.5). In the absence of S-HTC, only methanol acted as MW absorber since OA interacted poorly with MW. The OA conversion was achieved only 28%. It might say that MW alone is not capable of increasing the the reaction process conversion under this condition. While in the presence of 5 wt% of S-HTC under MW system was found 80.5% OA conversion. As a results, the catalytic activity of S-HTC was proved to have a potential catalyzed esterification due to the Brønsted acid sites of sulfonic (-SO₃H) which was confirmed the sulfur elements and functional group by elemental analysis and FT-IR spectra, respectively. Moreover, S-HTC also showed a strong MW radiation absorbing function due to polar molecules of sulfonic acid functionalization. The ability of S-HTC in absorbing MW energy and dissipating it into heat was also proved by dielectric loss tangent value ($\tan \delta=0.196$) at 2.45 GHz and 298 K. It is noted that the dielectric loss tangent observed in the work was in the same range as those reported in the literature for the carbonaceous material i.e. activated carbon, charcoal and carbon nanotube (0.11-0.80) at the same condition (Menendez et.al., 2010). Therefore, the synergism of S-HTC and MW can significantly accelerate the esterification reaction. The OA conversion increased to

93.3% when S-HTC and hexane under MW were combined. The ability of hexane is to separate OAME from the reaction mixture whereby OAME is soluble in the non-polar phase so that hexane acts as a separator of the product after the reaction. It was demonstrated that the addition of hexane provided higher yield of OAME since it is simultaneously removed from the reaction zone thereby shifting the reaction equilibrium forward.

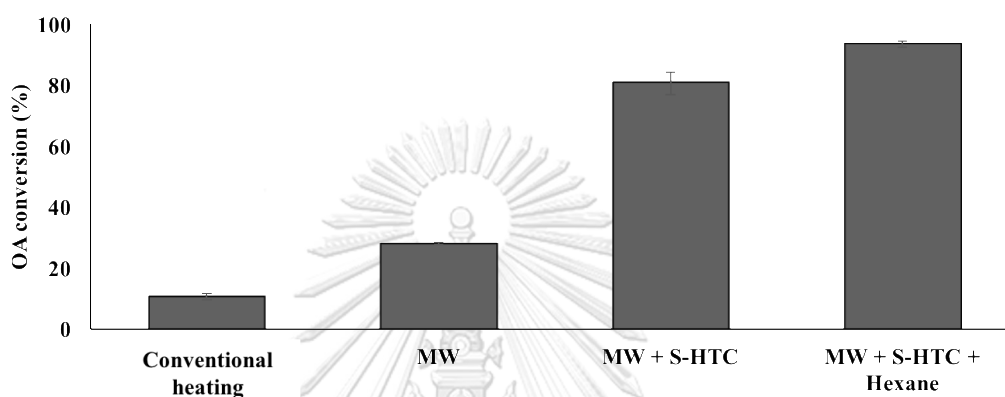


Figure 4.5 The parameters affecting the esterification reaction [Conditions: T=100°C, 60 min, OA to methanol 1:10, H/M=0.5 (v/v), 5wt% S-HTC and microwave power set = 300 W]

4.2.2 A single variable study

4.2.2.1 Effect of reaction temperature and time

The experiments were conducted using oleic acid and methanol with molar ratio of 1:10 in the presence of 1wt% catalyst loading and from 50-100°C for 30 min with hexane (Hexane/Methanol=1.8 v/v) as shown in Figure 4.6. This serves as a started operating condition unless otherwise specified. The OA conversion increases with the increase of reaction temperature due to higher rate of molecule movement and mass transfer rate. Next, the reaction time was evaluated from 30-60 min at 100°C in the presence of 1wt% catalyst loading with molar ratio of oleic to methanol at 1:10 and hexane to methanol ratio of 1.8 (v/v) as shown in Figure 2(b). The effect of reaction time is the same as reaction temperature where the OA conversion increases along with time.

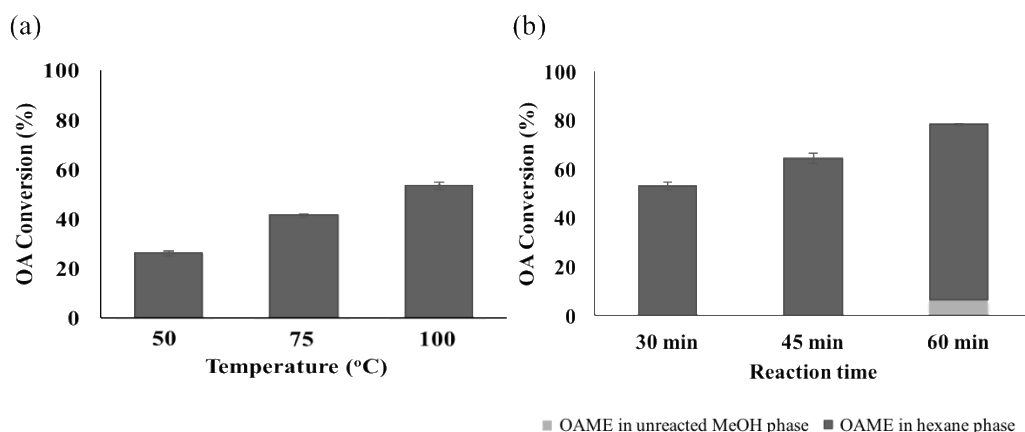


Figure 4.6 Results of esterification reaction under varied parameters (a) reaction temperature [Conditions: $t=30$ min, OA to methanol 1:10, H/M=1.8 (v/v), 1wt% catalyst loading and microwave power set = 300 W] and (b) reaction time. [Conditions: $T=100^{\circ}\text{C}$, OA to methanol 1:10, H/M=1.8 (v/v), 1wt% catalyst loading and microwave power set = 300 W]

4.2.2.2 Effect of molar ratio of oleic to methanol

The effect of molar ratio of oleic to methanol is one important variable affecting the esterification as shown in Figure 4.7. The OA conversion increased from 37 to 91% with an increase in the amount of methanol from 1:5 to 1:40 at $T = 100^{\circ}\text{C}$ for 60 min in the presence of 1wt% catalyst loading and hexane to methanol ratio of 1.8 (v/v). As expected, excessive usage of methanol was able to drive the equilibrium reaction forward. Moreover, OAME was found in both phases of the products (unreacted methanol phase and hexane phase) at the molar ratio of OA to methanol 1:10 and 1:25. Based on the results, the role of hexane as a separator could not show the efficiency when high amount of methanol. In short, the equilibrium can be shifted to produce more OAME by adding an excess methanol according to Le Charterlier's principle.

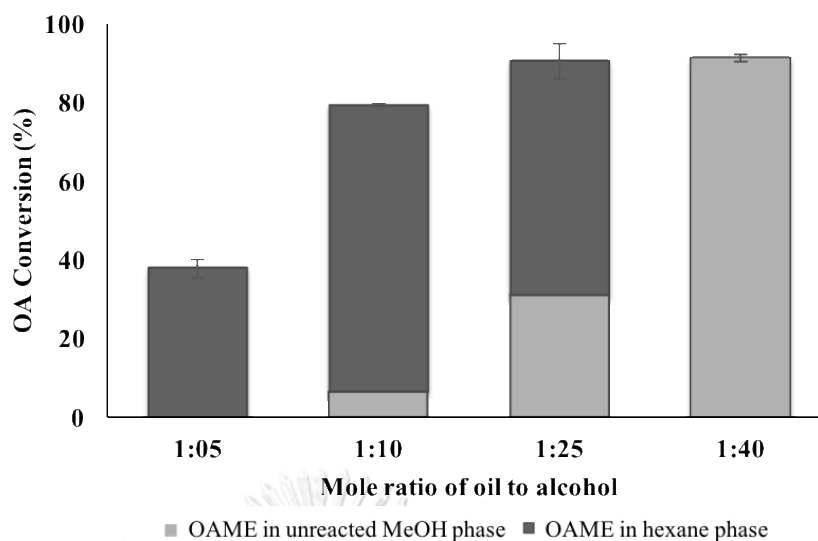


Figure 4.7 Effect of molar ratio of OA to methanol on esterification.

[Conditions: T=100°C, 60 min, Hexane amount=5 ml, 1wt% S-HTC and microwave power set=300 W]

4.2.2.3 Effect of catalyst loading

According to the catalyst loading in Figure 4.8, it was found that the conversion increased with increasing the amount of S-HTC. However, it seems less significant on the OA conversion when the catalyst loading was further increased. Moreover, the effect of addition of hexane was studied at different molar ratio of 1:10 and 1:25 by varying the catalyst loading as shown in Figure 4.8 (a, b). Based on the results, the highest OA conversion was obtained at 100°C for 60 min, 1:25 molar ratio of OA to methanol and 10% S-HTC. The excessive use of methanol at 1:25 molar ratio of OA to methanol was able to achieve high yield as expected and mentioned before. In particular, about 30% OAME was found in methanol phase under 1:25 molar ratio of OA to methanol. The result might be the same as the reports of Sajjadi et al. (2014) and Yuan et al. (2009), the excess methanol will lead to biodiesel and glycerol (polar molecules) being miscible. These indicated that high amount of methanol can lead a solubility of biodiesel and methanol.

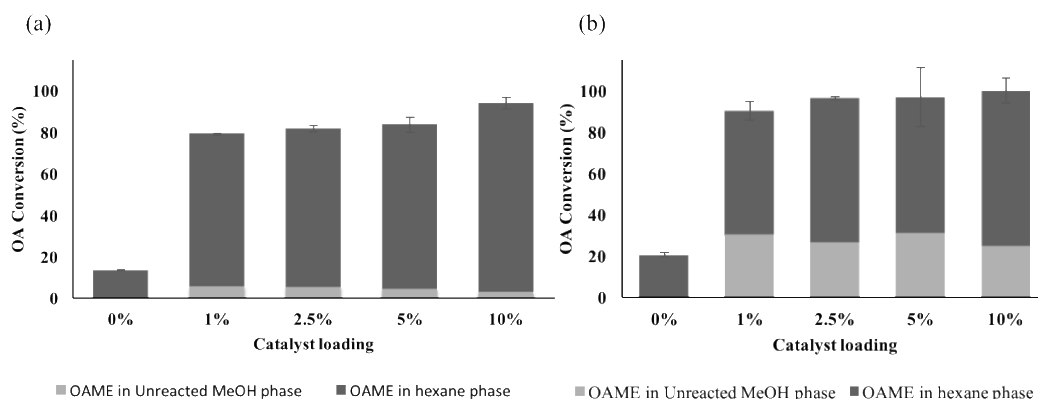


Figure 4.8 Effect of catalyst loading on esterification at molar ratio of OA to methanol 1:10 (a) and 1:25 (b). [Conditions: $T=100^{\circ}\text{C}$, 60 min, $H/M=1.8$ (v/v) and microwave power set=300 W]

4.2.2.4 Effect of amount of hexane

The effect of hexane was demonstrated in Figure 4.9. The amount of hexane to methanol (v/v) was varied; for example, $H/M=0.5$ means the volume of hexane is half the volume of methanol. From the results, the usage of hexane showed that the OAME yield increases slightly when compared with no addition of hexane ($H/M=0$).

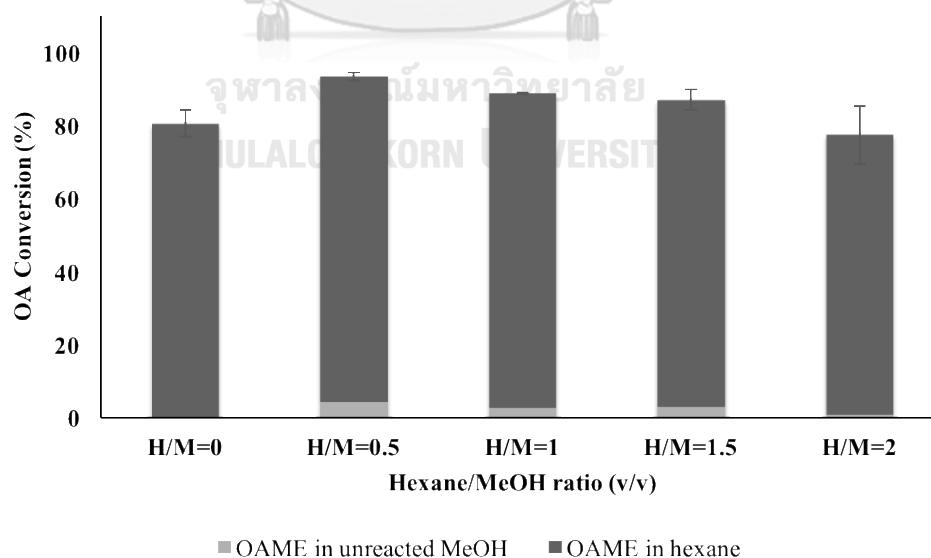


Figure 4.9 Effect of amount of hexane on esterification. [Conditions: $T=100^{\circ}\text{C}$, 60 min, OA to methanol 1:10,5 wt% catalyst loading and microwave power set = 300 W]

The increase in the amount of hexane added to the mixture was expected to give higher yield due to its role as a separator. Unfortunately, OA conversion decreased with increasing amount of hexane. It is likely that the excess amount of hexane could inhibit the reaction by shadowing the acid functionality of the catalyst, thereby hindering the reactants accessibility to the surface of the catalyst resulting to the lower yield. In summary, hexane as a separator might not be necessary in the system of S-HTC catalyzed esterification under microwave irradiation. Moreover, economic issue is concerned with the cost of production either cost of hexane and also the separation its from the target product. Therefore, the next experiments will be optimized and discussed in the system without hexane by using design of experiment.

4.3 Optimization of S-HTC catalyzed OA esterification conditions

4.3.1 Screening variables affecting OA esterification

The selection studies range of independent parameters was carried out by screening method. The influence of three parameters results namely, molar ratio of methanol to OA (1:1, 1:5, 1:10, 1:20), reaction time (15, 30, 45, 60 min) and catalyst loading (0, 1, 2.5, 5, 10 wt%) were presented in Figure 4.10-4.12. To investigate the actual parameter affecting the reaction, the other parameters were fixed at the lowest condition. For a stoichiometry esterification, the OA to methanol ratio is 1 and excessive usage of methanol is generally promoted the forward reaction since the esterification is reversible. Figure 4.10 investigated the effect of OA to methanol ratio, between 1:1 and 1:5 was shown the obviously increasing OA conversion. While the effect of reaction time was observed the changing between 45 and 60 min (Figure 4.11). In Figure 4.12, the catalyst loading represented ambiguously effect in this condition due to the low molar ratio and reaction time. However, the range of 1.5-3.5 wt% was chosen for optimization regarding economic consideration. As the results, 3 levels of CCD at low, middle and high, designated as -1, 0 and +1 respectively, are demonstrated in Table 3.1 to design of experiment.

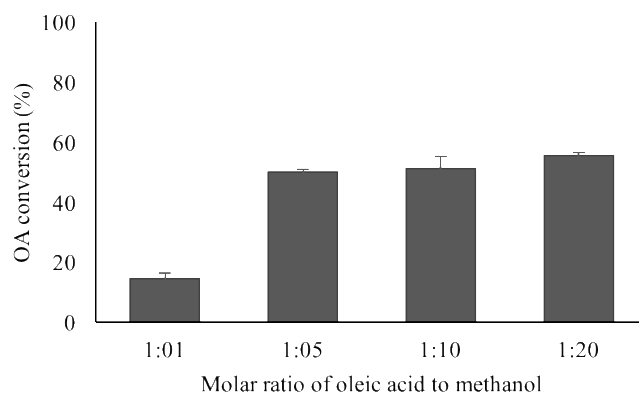


Figure 4.10 Effect of molar ratio of OA to methanol on esterification. [Conditions: T=100°C, 15 min, 1wt% catalyst loading and microwave power set = 300 W]

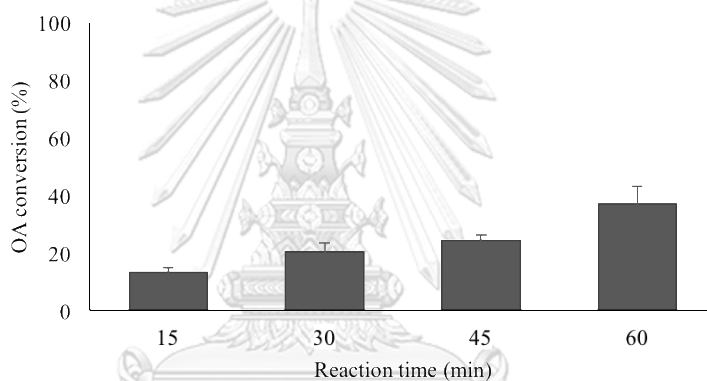


Figure 4.11 Effect of reaction time on esterification. Conditions: T=100°C, OA to methanol 1:1, 1wt% catalyst loading and microwave power set = 300 W]

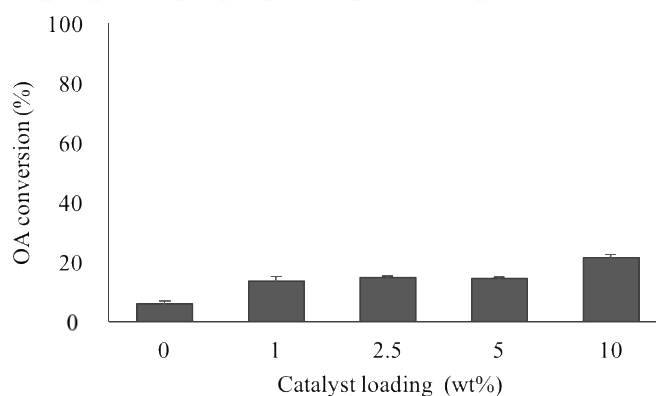


Figure 4.12 Effect of catalyst loading on esterification [Conditions: T=100°C, OA to methanol 1:1 and microwave power set = 300 W]

4.3.2. Design of experiment, quadratic regression model and variance analysis

The experiment of S-HTC catalyzed esterification was designed using RSM provided by Expert Design version 10. The experimental operating conditions and their corresponding OA conversions (responses) as well as the model predicted results are displayed in Table 4.2. The OA conversions ranged from 32.14% to 94.55%. The quadratic model, which includes all the independent variables and their binary interactions, is expressed as follows.

$$\text{OA conversion (\%)} = -62.44446 + 21.93250A + 1.27526B + 27.63576C - 0.078850AB - 0.38050AC + 0.17087BC - 1.30515A^2 - 0.00847B^2 - 5.66643C^2 \quad (9)$$

where A, B and C are the actual values of the methanol to OA molar ratio, reaction time and catalyst loading, respectively. The coefficient of regression (R^2) was used to fit the data for the quadratic polynomial equation. Based on R^2 of 0.9407 obtained, it is suggested that the prediction of the response was able to cover more than 90% of the variability in the experiments. The satisfactory prediction of OA conversion based on regression model as compared to the actual experimental data is shown in Figure 4.13. The statistical significance of each parameter was evaluated by the analysis of variance (ANOVA) (as presented in Table 4.3). The significance of each term in equation (9) was assessed by its corresponding p-value. At 95% of confidence level (p-value < 0.05), it can be revealed that A, C, A^2 and C^2 are significant. Moreover, the insignificant lack of fit confirmed that the quadratic model provides a satisfactory prediction of OA conversion.

Table 4.2 CCD variables for S-HTC catalyzed esterification and experimental (response) and predicted percent OA conversions.

Experi mental run	Methanol to OA molar ratio	Reaction time (min)	Catalyst loading (wt %)	Response % OA Conversion	Predicted % OA Conversion
1	2.5	50	1.5	59.68	55.41
2	7.5	50	1.5	78.39	72.95
3	2.5	70	1.5	68.84	58.77
4	7.5	70	1.5	76.25	77.76
5	2.5	50	3.5	74.95	68.71
6	7.5	50	3.5	86.44	82.88
7	2.5	70	3.5	87.53	80.41
8	7.5	70	3.5	94.55	96.02
9	0.8	60	2.5	47.08	47.03
10	9.2	60	2.5	85.48	74.88
11	5	43.1	2.5	83.37	81.97
12	5	76.8	2.5	90.54	95.99
13	5	60	0.8	60.18	61.91
14	5	60	4.2	86.47	88.70
15	5	60	2.5	91.85	91.54
16	5	60	2.5	93.36	91.54
17	5	60	2.5	89.99	91.54

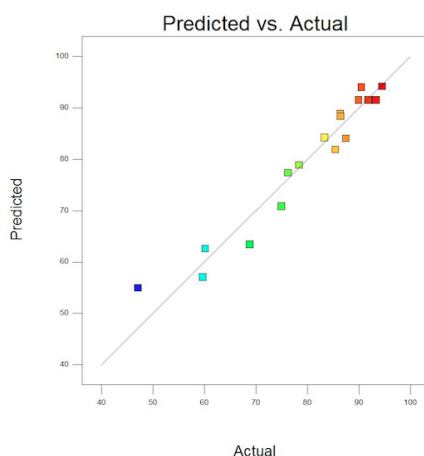


Figure 4.13 Comparison between the predicted and actual OA conversion

Table 4.3 Analysis of variance (ANOVA) for response surface quadratic model.

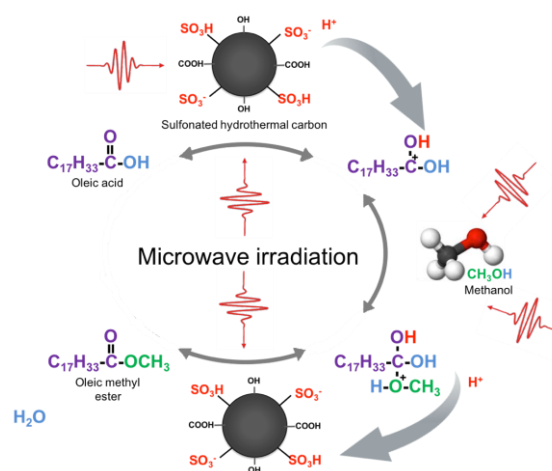
Source	Sum of Squares	Degree of freedom	Mean Square	F-value	p-value
Model	2801.16	9	311.24	12.35	0.0016*
A-Methanol to OA	873.33	1	873.33	34.65	0.0006*
B-Reaction time	115.80	1	115.80	4.59	0.0693
C-Catalyst loading	799.99	1	799.99	31.74	0.0008*
AB	31.09	1	31.09	1.23	0.3034
AC	7.24	1	7.24	0.29	0.6086
BC	23.36	1	23.36	0.93	0.3678
A ²	750.13	1	750.13	29.76	0.0010*
B ²	8.10	1	8.10	0.32	0.5886
C ²	361.97	1	361.97	14.36	0.0068*
Residual	176.43	7	25.20		
Lack of Fit	170.73	5	34.15	11.98	0.0788
Pure error	5.70	2			
Corrected total	4216.23	16			
R ²	0.9407				
Adj-R ²	0.8646				

*Parameters that significantly affect the reaction (p-value less than 0.05)

4.3.3. Effect of variables on OA conversion

The effect of molar ratio of methanol to OA, reaction time and catalyst loading on OA conversion are presented in 3D response surface plots as shown in Figure 4.14. The lowest p-value of 0.0006 and the correspondingly largest F-value of 34.65 indicate that molar ratio of methanol to OA was the most influential factor on OA conversion. This was followed by catalyst loading (Table 4.3).

It can be seen from Figure 4.14 (a,b) that the OAME production favored high molar ratio of OA to methanol. In an equilibrium reaction such as OA esterification, excessive of methanol forced the reaction toward the production of OAME. This was also seen in the result of OA conversion, which increased with increasing methanol to OA molar ratio from 2.5 to 7.5. The reaction time, on the other hand, showed negligible effect on OA conversion within the range studied (Figure 4.14 (b,c)). The effect of catalyst loading (%w/w) is presented in Figure 4.14 (b,c). With increased amount of catalysts, the Brønsted acid sites: (-SO₃H) and (-COOH), were also increased and the OA conversion was promoted. The mechanism of MW assisted esterification can be represented in Scheme 4.2, in which Brønsted acid, H⁺ protonated the carboxylic end of OA at the double bond position of carbon. Then methanol attacked on the carbonation leading to a tetrahedral intermediate. The OAME was then produced with the elimination of water, and the H⁺ was regenerated again at the surface of HTC catalyst (Lieu et al., 2016, Zeng et al., 2012, Kirk-Othmer Encyclopedia of Chemical Technology (4th Edition)).



Scheme 4.2. Mechanism of S-HTC catalyzed esterification under MW.

4.3.4. Optimization of OA conversion

The RSM analyses provided the prediction of the optimal conditions for OA conversion to be at 5.831:1 molar ratio of methanol to OA, 60 min and 3.047 wt% catalyst loading, yielding 95.55% OA conversion. The accuracy of the model prediction was confirmed by experiments, carried out under the RSM optimized condition. The experimental OA conversion of 92.76% was obtained, which was a 2.79% deviation from the model prediction. This result therefore suggested that the model is in good agreement with the experimental study. As far as the economic consideration is concerned, despite the suggested optimal condition, lower catalyst loading and molar ratio of OA to methanol of 2.5 wt% and 4.5:1, respectively, was found to give relatively high OA conversion of 90%, as seen t in Fig. 4.14 (b).

In addition, the S-HTC catalyzed esterification under MW irradiation were compared based on literature survey conducted esterification of oleic acid with different acid catalyst either homogeneous and heterogeneous catalysts under conventional heating as shown in Table 4.4. It clearly showed that the combination of alternative heating source of MW and S-HTC promoted an acceleration of the reaction rate. The fast reaction rate of the MW-assisted esterification was due to radiation directly pass through the vessel walls into the selected materials in the bulk mixture and resulted in molecular mobility and rapid heat in the reaction.

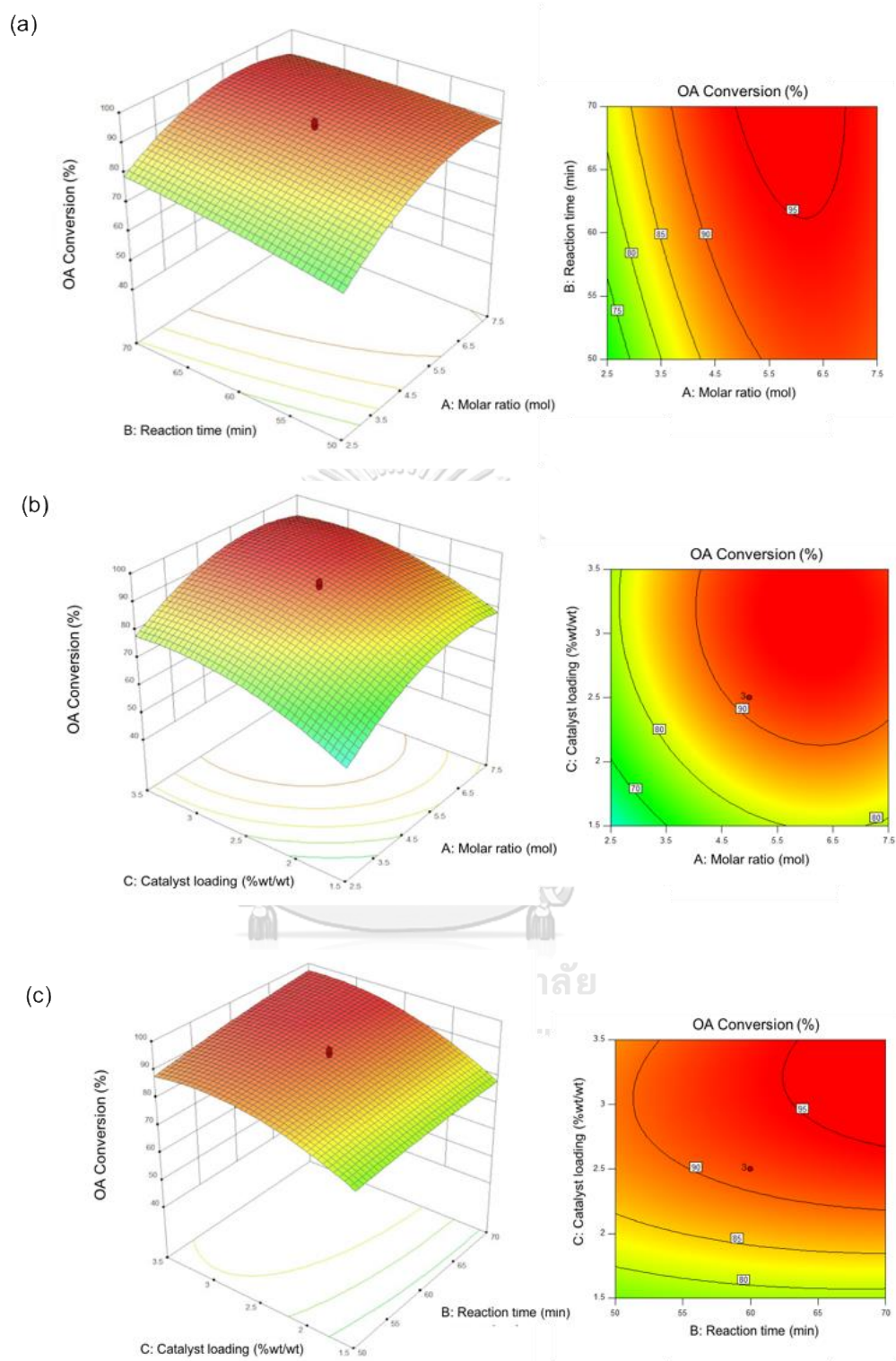


Figure 4.14 3-D response surface and contour plots representing effects of pairs of variables: (a) methanol to OA and reaction time; (b) methanol to OA and catalyst loading; and (c) reaction time and catalyst loading, on OA conversion.

Table 4.4 Comparison of the different acid catalysts on esterification reaction

Feedstock	Catalyst	MeOH:OA molar ratio	Reaction temperature (°C)	Reaction time (h)	Performance	Note	Ref.
Oleic acid	H ₂ SO ₄	3:1	80	6	91.5% conversion	Conventional heating with reflux	Park et al., 2010
Oleic acid	HCl	6:1	60	2	87.9% conversion	Conventional heating with reflux	Farag et al., 2011
Oleic acid	Sulfated zirconia (0.5 g)	40:1	60	12	90% yield	Conventional heating with reflux	Petal et al., 2013
Oleic acid	Sulfated LaO (10 wt%)	5:1	100	7	96% conversion	Conventional heating	Vieira et al., 2013
Oleic acid	Chlorosulfonic zirconia (3 wt%)	8:1	100	7	100% yield	Conventional heating	Zhang et al., 2014
Oleic acid	Sulfonated, carbonized D-glucose (5 wt%)	10:1	80	5	>95% yield	Conventional heating	Marchetti et al., 2008
Oleic acid	CH-A Cation exchange resins (20 g)	9:1 (EtOH)	82	8	93% conversion	Conventional heating	Jiang et al., 2013
Oleic acid	HZSM-5 (10 wt%)	20:1	60	10	86% conversion	Conventional heating	Vieira et al., 2013
Oleic acid	Sulfonated hydrothermal carbon (3 wt%)	5.8:1	100	1	92.8% conversion	Microwave heating	*This study

4.4. Kinetics study of S-HTC catalyzed esterification

4.4.1. Determination of kinetic parameters

To identify the kinetics of the reaction, experiments were carried out at different temperatures and times, and the results are shown in Figure 4.15. The OA conversion was found to increase with reaction time. It should be noted here that the OA conversion reached around 40%, the instant that the temperature of the reaction system reached the desired temperature, at which point, $t = 0$ min.

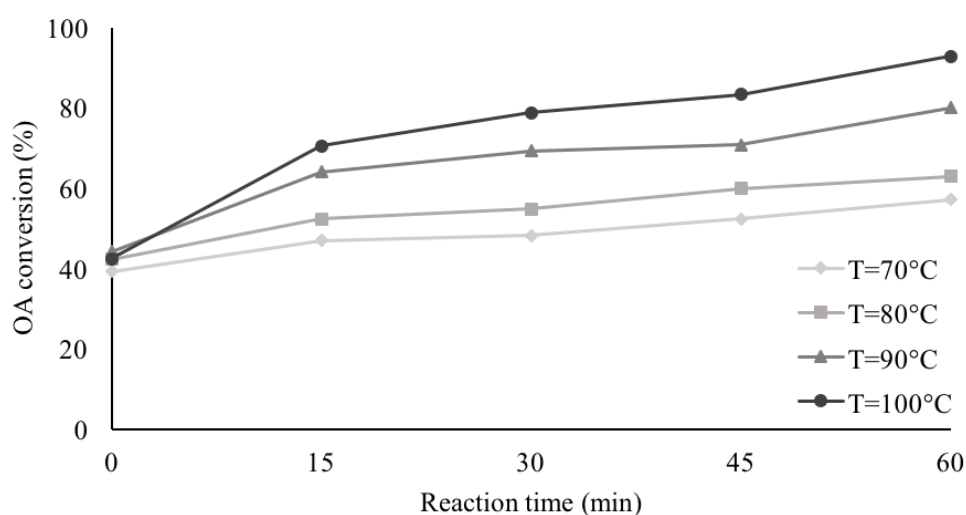


Figure 4.15 OA conversion as a function of time at different temperatures.

[Conditions: methanol to OA molar ratio = 5.831:1, 3.047 wt% catalyst loading and microwave power set = 300 W]

The reaction rate constant for respective temperature was determined based on Eq. (6) by plotting graph of $\ln(1-X_A)$ versus reaction time. The corresponding plot is displayed in Figure 4.16, while Table 4.4 summarizes the values of reaction rate constants at different temperatures. High coefficient of determinations (R^2) were observed, thus the assumption of pseudo-first order reaction kinetic was verified. The rate constants increased with the increasing reaction temperatures from 70°C to 100°C due to the endothermic reaction nature of esterification, suggesting also that the forward reaction was accelerated by the increase in reaction temperature.

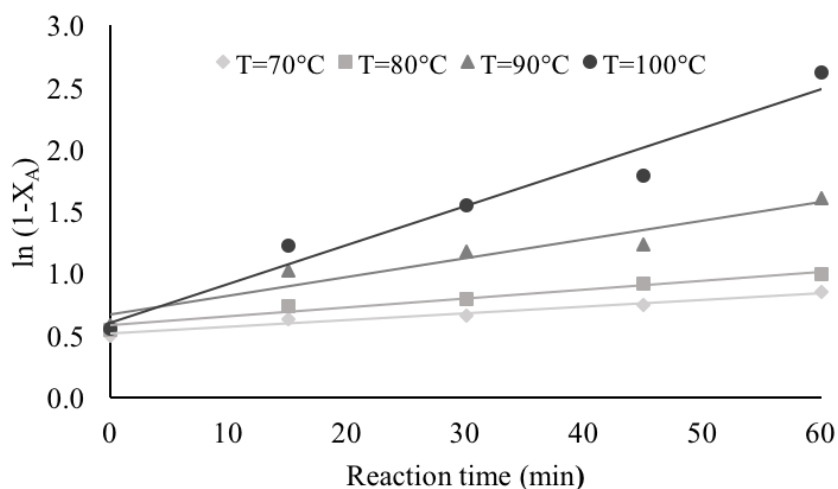


Figure 4.16 Kinetic plot for determination of reaction rate constants.

Table 4.4. Reaction rate constants for S-HTC catalyzed OA esterification.

Temperature (°C)	Reaction rate constant, k (min^{-1})	Coefficient of determination (R^2)
70	0.0054	0.9627
80	0.0071	0.9654
90	0.0151	0.9246
100	0.0315	0.9598

4.4.2. Arrhenius plot and activation energy

As shown in Figure 4.17, the relation of $\ln k$ and $1/T$ was plotted to determine the activation energy and the frequency factor based on the Arrhenius equation. The activation energy for the S-HTC catalyzed esterification of OA was found to be 64 kJ/mol. It is noted that the activation energy observed in the work was in the same range as those reported in the literature for the esterification reaction catalyzed by several acid compounds i.e. H_2SO_4 , Aminophosphonic acid resin, Cation exchange resin/polyethersulfone and NaY Zeolite (42-73 kJ/mol) (Lie et al., 2016; Liu et al., 2013; Zhang et al., 2012; Abbas et al., 2013). While the frequency factor of $2.58 \times 10^7 \text{ min}^{-1}$ was observed that higher than the conventional heating (Lieu et al., 2016) It is due to the increasing of the molecular mobility under MW field.

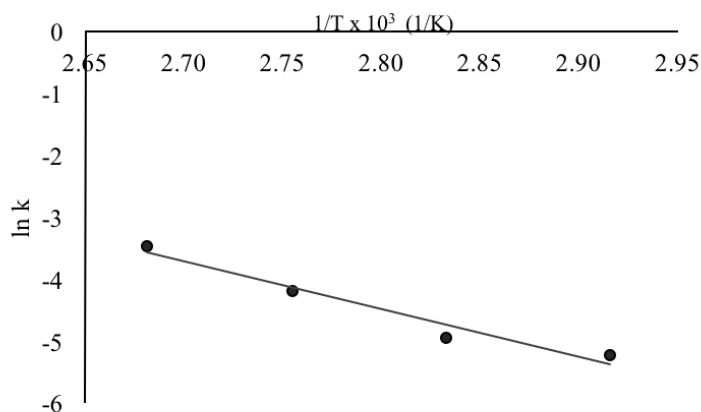


Figure 4.17 Arrhenius plot for estimation on activation energy and frequency factor.

4.5. Stability, reusability and spent catalyst characterization of S-HTC

In order to study the stability of sulfonic groups and possibility of catalyst reuse, the catalytic activity of S-HTC was evaluated. The catalyst was repeatedly used for the esterification reaction of OA and methanol under MW irradiation under the same condition (optimum condition). The S-HTC was filtered and washed with methanol and hexane, then reused in the new reaction runs. As the results in Figure 4.18, the OA conversion decreased from 93% to 20% in five consecutive cycles. The OA conversion decreased instantly according to the catalyst is not active after first run.

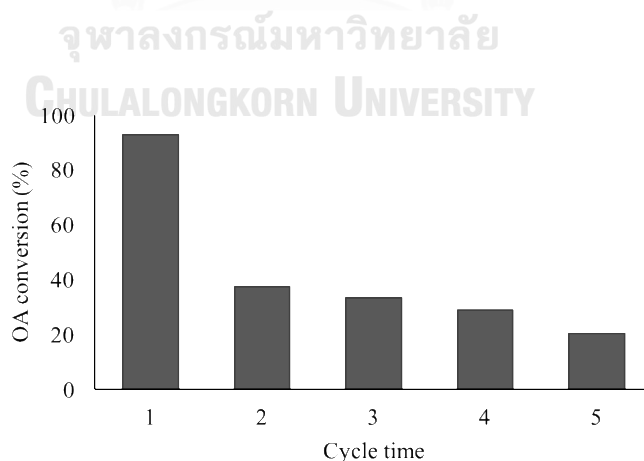


Figure 4.18 Reusability of S-HTC in esterification under the optimal condition.

[Conditions: methanol to OA molar ratio = 5.831:1, 3.047 wt% catalyst loading and microwave power set = 300 W]

The suspected reason for the decreasing OA conversion after reusing S-HTC was leaching of sulfonic groups from the latter. Even though, the sulfonic groups or the main active sites for the biodiesel production will still be present in the reaction solution. Hence, we expected to get high OA conversion. According to Jose M., et al., 2012, another possibility is that the sulfonic groups deactivated. Sulfonic acid might be changed to sulfonate ester after the reaction with alcohol which is also present in the reaction mixture.



CHAPTER V

CONCLUSIONS AND RECOMMENDATIONS

5.1 Conclusions

S-HTC was successfully catalyzed esterification of OA and methanol under MW irradiation by using green and environmental friendly preparation. The synergism of S-HTC and microwave irradiation has been successfully performed a good microwave-absorptivity of at least two Brønsted acid sites, namely the -COOH and -SO₃H groups. The ability of hexane to separate OAME from the reaction mixture and to shift the reaction equilibrium forward was observed at 0.5 hexane to methanol volume ratio. An excess hexane could not give higher OAME as expected. Hexane might inhibit the reaction by shadowing the acid functionality of the catalyst.

RSM based on CCD was employed for the prediction and the optimization of OA conversion of the of S-HTC catalyzed OA esterification. Within the range of conditions studied, the molar ratio of methanol to OA was shown be the most influential factor on the OA conversion, followed by catalyst loading. On the other hand, reaction time showed negligible effect on OA conversion. The RSM analyses provided the prediction of the optimal conditions for OA conversion to be at 5.831:1 molar ratio of methanol to OA, 60 min and 3.047 wt% catalyst loading, yielding 95.55% OA conversion. The accuracy of the model prediction was confirmed by experiments, OA conversion of 92.76% was obtained, which was a 2.79% deviation from the model prediction. This result therefore suggested that the statistical model is in good agreement with the coefficient of regression (R^2) of 0.9407.

Furthermore, the reaction was found to be reasonably described by the pseudo-first order kinetics. The dependency of the reaction rate constant on temperatures gave the value of the activation energy of 64 kJ/mol. Unfortunately, the recyclability of S-HTC presented the decreasing in OA conversion rapidly after first run maybe due to the sulfonic groups deactivated.

5.2 Recommendations

From this research, the hypothesis of using S-HTC accelerated esterification was successfully produced OAME. Unfortunately, the catalyst reusability was proved that this catalyst should be improved the stability due to the catalyst reactivity rapidly dropped in the second cycle. According to related literatures in esterification, the main reasons of catalyst deactivation of sulfonated carbon have been reported by leaching of sulfonic species in sulfated zirconia (Tian et al., 2011) and formation of sulfonic esters with corresponding alcohol (Fraile et al., 2012). However, the deactivation is complicated phenomenon related to process which depends on the catalyst and catalytic reaction. There are recommendations to investigate and further study for improvement of S-HTC stability.

(i) The leaching of sulfonic groups will be studied by dissolving S-HTC in methanol and heat at required reaction temperature for required reaction time. Then test the acidity in the solution and test the activity of that catalyst in the esterification to confirm the stability of acid site of catalyst (Zhao et al., 2016). If the leaching happen, the acid functionalization step should be modified.

(ii) The forming of sulfonic esters will be carried out by analyzing spent catalyst (after test the activity in the reaction) such as FTIR and ^{13}C NMR.

Moreover, the hypothesis of using hexane for removing the product from the reaction phase, the results could not clearly show the role of a separator of hexane. In addition, the interaction effect between methanol (reactant) and hexane (separator) need to further investigate by using design of experiment. Phase equilibrium of mixture also need to consider in further study.

Lastly, the effect of thermal and non-thermal MW is an important issue to describe the phenomenon effect during the reaction under MW irradiation. Non-thermal effects are the interaction between dipolar molecules and charges in electric field (Mazo et al., 2011). Therefore, if frequency factor A of the Arrhenius equation in MW heating is higher than that conventional heating and activation energy in MW heating is lower than conventional heating. The collision efficiency can be lead to

accelerate in the reaction and that means the non-thermal effect of MW. Also the MW power is one parameter which might affect to the reaction. Therefore, open system and closed system might be needed to compare the different type of MW. Energy requirement is needed to calculate and compare to the conventional heating.



APPENDIX A EXPERIMENTAL DATA FOR ANALYSIS

A1 Standard calibration curve

Table A-1.1: Standard data of methyl oleate (MO) and 2,6- dimethylnaphthalene (DMN) as an internal standard.

Standard	Concentration (mg/l)	Peak area
DMN	0.5	428,606.4
MO	800	264,224.6
DMN	0.5	421,624.4
MO	1600	393,241.1
DMN	0.5	428,648.2
MO	3200	862,870.6
DMN	0.5	399,519.4
MO	6400	3,070,301.2
DMN	0.5	419,202.0
MO	12800	7,257,898.8
DMN	0.5	388,389.0
MO	25600	14,410,530.8

The response factor (RF) is a measure of the relative mass spectral response of MO compared to DMN. It is calculated by using the reference MO standard as shown in equation A-1. C is concentration, and A is peak area.

$$RF = \frac{C_{MO}/C_{DMN}}{A_{MO}/A_{DMN}} \quad (A-1)$$

where

C_{MO} = methyl oleate standard concentration (mg/l)

C_{DMN} = 2,6- dimethylnaphthalene concentration (mg/l)

A_{MO} = methyl oleate standard peak area

A_{DMN} = 2,6- dimethylnaphthalene peak area

Table A-1.2: The relationship between concentration and peak area on RF

C_{MO}/C_{DMN}	A_{MO}/A_{DMN}
800	0.6165
3200	0.9327
6400	2.0130
12800	7.6850
25600	17.3136
51200	37.1033

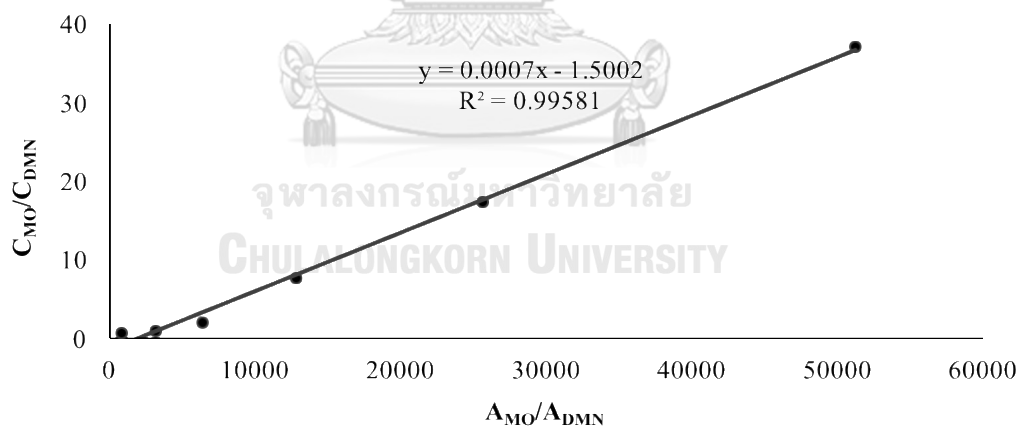


Figure A-1 Standard calibration curve of methyl oleate

A2 Calculation of the OA conversion

The percentage of oleic acid methyl ester is defined as

$$\% \text{ OA Conversion} = \frac{\text{mol of OAME}}{\text{mol of OA}} \times 100 \quad (\text{A-2})$$

Mol of OAME is calculated as

$$\text{mol of OAME} = \frac{\text{weight of OAME}}{\text{MW of OA}} \quad (\text{A-3})$$

Weight of OAME is computed as

$$\text{weight of OAME} = \frac{C_{\text{OAME}} \times V_{\text{OAME}} \times \text{DF}}{1000} \quad (\text{A-4})$$

Concentration of OAME is calculated as

$$C_{\text{OAME}} = \frac{\text{RF} \times C_{\text{DMN}} \times A_{\text{OAME}}}{A_{\text{DMN}}} \quad (\text{A-5})$$

where

C_{OAME} = oleic acid methyl ester concentration (mg/l)

V_{OAME} = oleic acid methyl ester volume (ml)

A_{OAME} = oleic acid methyl ester peak area

DF = dilution factor

APPENDIX B

EXPERIMENTAL DATA

B1 Catalytic activity

Table B-1: The catalytic activity preliminary results of S-HTC. [Conditions: T=100°C, 60 min, OA to methanol 1:10, 5wt% catalyst loading and microwave power set = 300 W]

Condition	OA conversion (%)			SD
	Exp.1	Exp.2	Avg.	
Control exp.	11.48	10.04	10.76	1.02
MW	28.11	28.68	28.40	0.40
MW + S-HTC	79.18	84.27	81.73	3.60

B2 Screening parameters effect

Table B-2.1: Effect of molar ratio to methanol on esterification. Conditions: T=100°C, 15 min, 1wt% catalyst loading and microwave power set = 300 W]

Molar ratio of OA to methanol	OA conversion (%)			SD
	Exp.1	Exp.2	Avg.	
1:1.	15.85	13.33	14.59	1.78
1:5	50.03	49.89	49.96	0.87
1:10	48.67	54.13	51.40	3.86
1:20	54.97	56.24	55.61	0.90

Table B-2.2: Effect of reaction time on esterification. Conditions: T=100°C, OA to methanol 1:1, 1wt% catalyst loading and microwave power set = 300 W]

Reaction time (min)	OA conversion (%)			SD
	Exp.1	Exp.2	Avg.	
15	14.57	12.26	13.41	1.64
30	18.47	22.58	20.52	2.91
45	22.98	25.73	24.36	1.94
60	32.79	41.56	37.18	6.20

Table B-2.3: Effect of catalyst loading on esterification n. Conditions: T=100°C, OA to methanol 1:1 and microwave power set = 300 W]

Catalyst loading (wt%)	OA conversion (%)			SD
	Exp.1	Exp.2	Avg.	
0	5.18	6.71	5.94	1.08
1	14.57	12.26	13.41	1.64

B3 Design of experiment

Table B-3: RSM based on CCD experimental for S-HTC catalyzed esterification conversions. [Conditions: T=100°C and microwave power set = 300 W]

Experimental run	OA conversion (%)		Catalyst loading (wt %)	SD
	Exp.1	Exp.2		
1	60.72	58.64	59.68	1.47
2	81.31	75.47	78.39	4.13
3	67.95	69.73	68.84	1.26
4	74.13	78.37	76.25	3.00
5	74.75	75.15	74.95	0.28
6	80.11	92.77	86.44	8.95
7	88.91	86.15	87.53	1.95
8	92.01	97.09	94.55	3.59
9	53.65	40.51	47.08	9.29
10	83.82	87.14	85.48	2.35
11	83.76	82.98	83.37	0.55
12	92.70	88.38	90.54	3.05
13	55.91	64.45	60.18	6.04
14	87.19	85.75	86.47	1.02
15	94.52	89.18	91.85	3.78
16	90.67	96.05	93.36	3.80
17	91.86	88.12	89.99	2.64

B4 Kinetics study

Table B-4: OA conversion as a function of time at different temperatures. [Conditions: methanol to OA molar ratio = 5.831:1, 3.047 wt% catalyst loading and microwave power set = 300 W]

Temperature (°C)	OA conversion (%)				
	0 min	15 min	30 min	45 min	60 min
70	39.16	46.98	48.18	52.36	57.16
80	42.19	52.24	54.78	59.92	62.95
90	44.15	64.01	69.26	70.80	80.00
100	42.41	70.46	78.77	83.33	92.76

B5 Reusability

Table B-5 Reusability of S-HTC in esterification under the optimal condition. [Conditions: methanol to OA molar ratio = 5.831:1, 3.047 wt% catalyst loading and microwave power set = 300 W]

Catalyst	OA conversion (%)
Fresh catalyst	92.76
1 st reuse	37.37
2 nd reuse	33.21
3 rd reuse	28.87
4 th reuse	20.38

REFERENCES

- Arancon, R.A., Barros, H.R., Balu, A.M., Vargas, C., & Luque, R. (2011). Valorisation of corncob residues to functionalised porous carbonaceous materials for the simultaneous esterification/transesterification of waste oils. *Green Chemistry*, 13, 3162–3167.
- Ardizzone, S. , Bianchi, C. L. , Cappelletti, G. , & Porta, F. (2004) . Liquid-phase catalytic activity of sulfated zirconia from sol– gel precursors: the role of the surface features. *Journal of Catalysis*, 227(2), 470-478.
- Ashrafi, B. , Díez- Pascual, A. M. , Johnson, L. , Genest, M. , Hind, S. , Martinez- Rubi, Y. , Johnston, A. (2012) . Processing and properties of PEEK/ glass fiber laminates: Effect of addition of single- walled carbon nanotubes. *Composites Part A: Applied Science and Manufacturing*, 43(8), 1267-1279.
- Atribak, I. , Such- Basáñez, I. , Bueno- López, A. , & García, A. (2007). Comparison of the catalytic activity of MO₂ (M= Ti, Zr, Ce) for soot oxidation under NO_x/ O₂. *Journal of Catalysis*, 250(1), 75-84.
- Atta- Obeng, E., Dawson- Andoh, B., Felton, E., & Dahle, G. (2018). Carbon Dioxide Capture Using Amine Functionalized Hydrothermal Carbons from Technical Lignin. *Waste and Biomass Valorization*.
- Atwater, J.E., & Wheeler, R.R. (2003). Complex permittivities and dielectric relaxation of granular activated carbons at microwave frequencies between 0.2 and 26 GHz. *Carbon*, 41, 1801-1807.
- Atwater, J.E., & Wheeler, R.R. (2004). Temperature dependent complex permittivities of graphitized carbon blacks at microwave frequencies between 0.2 and 26 GHz. *Journal of Materials Science*, 39, 151-157.
- Aviara, N. A., Power, P. P., & Abbas, T. (2013). Moisture- dependent physical properties of *Moringa oleifera* seed relevant in bulk handling and mechanical processing. *Industrial Crops and Products*, 42, 96-104.

- Bet- Moushoul, E., Farhadi, K., Mansourpanah, Y., Nikbakht, A. M., Molaei, R., & Forough, M. (2016). Application of CaO- based/ Au nanoparticles as heterogeneous nanocatalysts in biodiesel production. *Fuel*, 164, 119-127.
- Bezerra, M. A., Santelli Re Fau - Oliveira, E. P., Oliveira Ep Fau - Villar, L. S., Villar Ls Fau - Escaleira, L. A., & Escaleira, L. A. Response surface methodology (RSM) as a tool for optimization in analytical chemistry. (1873- 3573 (Electronic)).
- Boey, P. - L., Ganesan, S., Maniam, G. P., Khairuddean, M., & Efendi, J. (2013). A new heterogeneous acid catalyst for esterification: Optimization using response surface methodology. *Energy Conversion and Management*, 65, 392-396.
- Challa, S., Little, W.E., & Cha, C.Y. (1994). Measurement of the dielectric properties of char at 2.45 GHz. *Journal of Microwave Power and Electromagnetic Energy*, 29, 131-137.
- Chen, H., & Wang, J. F. (2006). Biodiesel from Transesterification of Cottonseed Oil by Heterogeneous catalysis. In H. - K. Rhee, I. - S. Nam, & J. M. Park (Eds.), *Studies in Surface Science and Catalysis* (Vol. 159, pp. 153-156): Elsevier.
- Chouard, N., Caurant, D., Majérus, O., Guezi- Hasni, N., Dussossoy, J. - L., Baddour-Hadjean, R., & Pereira- Ramos, J. - P. (2016) . Thermal stability of SiO₂- B₂O₃- Al₂O₃- Na₂O- CaO glasses with high Nd₂O₃ and MoO₃ concentrations. *Journal of Alloys and Compounds*, 671, 84-99.
- Chuah, L. F. , Klemeš, J. J. , Yusup, S. , Bokhari, A. , & Akbar, M. M. (2017) . A review of cleaner intensification technologies in biodiesel production. *Journal of Cleaner Production*, 146, 181-193.

- Chung, K.-H., & Park, B.-G. (2009). Esterification of oleic acid in soybean oil on zeolite catalysts with different acidity. *Journal of Industrial and Engineering Chemistry*, 15(3), 388-392.
- Demir- Cakan, R., Makowski, P., Antonietti, M., Goettmann, F., & Titirici, M. - M. (2010) . Hydrothermal synthesis of imidazole functionalized carbon spheres and their application in catalysis. *Catalysis Today*, 150(1), 115-118.
- Egres, A. G., Hatje, V., Miranda, D. A., Gallucci, F., & Barros, F. (2019). Functional response of tropical estuarine benthic assemblages to perturbation by Polycyclic Aromatic Hydrocarbons. *Ecological Indicators*, 96, 229-240.
- Fan, X., Yu, C., Ling, Z., Yang, J., & Qiu, J. (2013). Hydrothermal Synthesis of Phosphate- Functionalized Carbon Nanotube- Containing Carbon Composites for Supercapacitors with Highly Stable Performance. *ACS Applied Materials & Interfaces*, 5(6), 2104-2110.
- Fang, Z., Li, C., Sun, J., Zhang, H., & Zhang, J. (2007). The electromagnetic characteristics of carbon foams. *Carbon*, 45, 2873-2879.
- Farag, H.A., El-Maghraby, A., & Taha, N.A. (2011). Optimization of factors affecting esterification of mixed oil with high percentage of free fatty acid. *Fuel Processing Technology*, 92, 507–510.
- Fraile, J. M. , García- Bordejé, E. , & Roldán, L. (2012). Deactivation of sulfonated hydrothermal carbons in the presence of alcohols: Evidences for sulfonic esters formation. *Journal of Catalysis*, 289, 73-79.
- Granato, D. , de Araújo Calado, V. M. , & Jarvis, B. (2014). Observations on the use of statistical methods in Food Science and Technology. *Food Research International*, 55, 137-149.

- Guéret, C. , Billaud, F. , Fixari, B. , & Le Perchec, P. (1995). Thermal coupling of methane, experimental investigations on coke deposits. *Carbon*, 33(2), 159-170.
- Guerrero, E. D. , Marín, R. N. , Mejías, R. C. , & Barroso, C. G. (2006). Optimisation of stir bar sorptive extraction applied to the determination of volatile compounds in vinegars. *Journal of Chromatography A*, 1104(1), 47-53.
- Guo, F., Xiu, Z., & Liang, Z. (2012). Synthesis of biodiesel from acidified soybean soapstock using a lignin-derived carbonaceous catalyst. *Applied Energy*, 98,47–52.
- Hara, M. (2010) Biodiesel production by amorphous carbon bearing SO₃H, COOH and phenolic OH groups, a solid Brønsted acid catalyst. *Topics in Catalysis*, 53, 805–810.
- Hashemzahi, M. , Saghatoleslami, N. , & Nayebzadeh, H. (2017). Microwave-Assisted Solution Combustion Synthesis of Spinel- Type Mixed Oxides for Esterification Reaction. *Chemical Engineering Communications*, 204(4), 415-423.
- Hernández- Hipólito, P. , Juárez- Flores, N. , Martínez- Klimova, E. , Gómez- Cortés, A. , Bokhimi, X. , Escobar- Alarcón, L. , & Klimova, T. E. (2015). Novel heterogeneous basic catalysts for biodiesel production: Sodium titanate nanotubes doped with potassium. *Catalysis Today*, 250, 187-196.
- Hows, M. E. P. , Perrett, D. , & Kay, J. (1997). Optimisation of a simultaneous separation of sulphonamides, dihydrofolate reductase inhibitors and β -lactam antibiotics by capillary electrophoresis. *Journal of Chromatography A*, 768(1), 97-104.
- Islam, M. A. , Brown, R. J. , Brooks, P. R. , Jahirul, M. I. , Bockhorn, H. , & Heimann, K. (2015). Investigation of the effects of the fatty acid

profile on fuel properties using a multi- criteria decision analysis. *Energy Conversion and Management*, 98, 340-347.

Jalbani, N. , Kazi, T. G. , Arain, B. M. , Jamali, M. K. , Afridi, H. I. , & Sarfraz, R. A. (2006). Application of factorial design in optimization of ultrasonic- assisted extraction of aluminum in juices and soft drinks. *Talanta*, 70(2), 307-314.

Jiang, Y. , Lu, J. , Sun, K. , Ma, L. , & Ding, J. (2013). Esterification of oleic acid with ethanol catalyzed by sulfonated cation exchange resin: Experimental and kinetic studies. *Energy Conversion and Management*, 76, 980-985.

Jordão, C. P. , Fernandes, R. B. A. , de Lima Ribeiro, K. , de Souza Nascimento, B. , & de Barros, P. M. (2009). Zn (II) adsorption from synthetic solution and kaolin wastewater onto vermicompost. *Journal of Hazardous Materials*, 162 (2), 804-811.

Kansedo, J. , & Lee, K. T. (2012). Transesterification of palm oil and crude sea mango (*Cerbera odollam*) oil: The active role of simplified sulfated zirconia catalyst. *Biomass and Bioenergy*, 40, 96-104.

Kappe, C. O. , Stadler, A. , Dallinger, D. , Mannhold, R. , Kubinyi, H. , & Folkers, G. (2012). *Microwaves in organic and medicinal chemistry*. 2nd ed. Weinheim, Germany: Wiley-VCH.

Kim, D., Choi, J., Kim, G.J., Seol, S.K., Ha, Y.C., Vijayan, M., Jung, S., Kim, B.H., Lee, D. & Park, S.S. (2011). Microwave-accelerated energy-efficient esterification of free fatty acid with a heterogeneous catalyst. *Bioresource Technology*, 102 (3), 3639–3641.

Kim, D., Choi, J., Kim, G., Seol, S.K. & Jung, S. (2011). Accelerated esterification of free fatty acid using pulsed microwaves. *Bioresource Technology*, In press.

- Kim, M., DiMaggio, C. , Yan, S. , Wang, H. , Salley, S. O. , & Simon Ng, K. Y. (2011). Performance of heterogeneous ZrO₂ supported metaloxide catalysts for brown grease esterification and sulfur removal. *Bioresource Technology*, 102 (3) , 2380-2386.
- Klaewkla, R. , Arend, M. , & Hoelderich, W. (2011). A Review of Mass Transfer Controlling the Reaction Rate in Heterogeneous Catalytic Systems. *Mass Transfer - Advanced Aspects*, 667-684.
- Kostas, E., Beneroso, D., & P. Robinson, J. (2017). The application of microwave heating in bioenergy: A review on the microwave pre-treatment and upgrading technologies for biomass (Vol. 77).
- Lam, M. K., Lee, K. T. , & Mohamed, A. R. (2010). Homogeneous, heterogeneous and enzymatic catalysis for transesterification of high free fatty acid oil (waste cooking oil) to biodiesel: A review. *Biotechnology Advances*, 28(4), 500-518.
- Leung, D., & Guo, Y. (2006). Transesterification of neat and used frying oil: Optimization for biodiesel production (Vol. 87).
- Lieu, T., Yusup, S., & Moniruzzaman, M. (2016). Kinetic study on microwave- assisted esterification of free fatty acids derived from *Ceiba pentandra* Seed Oil. *Bioresource Technology*, 211, 248-256.
- Lin, H., Zhu, H., Guo, H., & Yu, L. (2008). Microwave-absorbing properties of Co-filled carbon nanotubes. *Materials Research Bulletin*, 43, 2697-2702.
- Liu, S., Shen, Q., Cao, Y., Gan, L., Wang, Z., Steigerwald, M. L., & Guo, X. (2010). Chemical functionalization of single-walled carbon nanotube field-effect transistors as switches and sensors. *Coordination Chemistry Reviews*, 254 (9), 1101-1116.
- Liu, T. , Li, Z. , Li, W. , Shi, C. , & Wang, Y. (2013). Preparation and characterization of biomass carbon-based solid acid catalyst for the

esterification of oleic acid with methanol. *Bioresource Technology*, 133, 618-621.

Liu, W. , Yin, P. , Liu, X. , Chen, W. , Chen, H. , Liu, C. , . . . Xu, Q. (2013). Microwave assisted esterification of free fatty acid over a heterogeneous catalyst for biodiesel production. *Energy Conversion and Management*, 76, 1009-1014.

Ma, F., & Hanna, M. A. (1999). Biodiesel production: a review. *Journal Series #12109, Agricultural Research Division, Institute of Agriculture and Natural Resources, University of Nebraska–Lincoln*. *Bioresource Technology*, 70(1), 1-15.

Ma, J., Fang, M., Li, P., Zhu, B., Lu, X., & Lau, N.T. (1997). Microwave-assisted catalytic combustion of diesel soot. *Applied Catalysis A*, 159, 211-228.

Ma, L., Lv, E., Du, L., Lu, J., & Ding, J. (2016). Statistical modeling/optimization and process intensification of microwave- assisted acidified oil esterification, 122.

Ma, Y., Liu, X., Yin, Y., Zou, C., Wang, W., Zou, S., & Zhang, M. (2015). Expression optimization and biochemical properties of two glycosyl hydrolase family 3 beta-glucosidases. *Journal of Biotechnology*, 206, 79-88.

Malins, K., Kampars, V., Brinks, J., Neibolte, I., & Murnieks, R. (2015). Synthesis of activated carbon based heterogenous acid catalyst for biodiesel preparation. *Applied Catalysis B: Environmental*, 176-177, 553-558.

Marchetti, J.M., & Errazu, A.F. (2008). Esterification of free fatty acids using sulfuric acid as catalyst in the presence of triglycerides. *Biomass Bioenergy*, 32, 892–895.

- Mardhiah, H. H. , Ong, H. C. , Masjuki, H. H. , Lim, S. , & Lee, H. V. (2017) . A review on latest developments and future prospects of heterogeneous catalyst in biodiesel production from non- edible oils. *Renewable and Sustainable Energy Reviews*, 67, 1225-1236.
- Marland, S., Merchant, A., & Rowson, N. (2001). Dielectric properties of coal. *Fuel*, 80, 1839-1849.
- Martinez- Guerra, E. , & Gude, V. G. (2014) . Transesterification of used vegetable oil catalyzed by barium oxide under simultaneous microwave and ultrasound irradiations. *Energy Conversion and Management*, 88, 633-640.
- Mazo, P., & Rios, L. (2010). Esterification and transesterification assisted by microwave of crude palm oil. Homogeneous catalysis. *Latin American Applied Research*, 40 (4), 337-342.
- Mazo, P., & Rios, L. (2010). Esterification and transesterification assisted by microwave of crude palm oil. Heterogeneous catalysis. *Latin American Applied Research*, 40 (4), 343-349.
- Mazo, P. , Rios, L. , Estenoz, D. , & Sponton, M. (2012) . Self- esterification of partially maleated castor oil using conventional and microwave heating. *Chemical Engineering Journal*, 185-186, 347-351.
- Meher, L. C. , Vidya Sagar, D. , & Naik, S. N. (2006) . Technical aspects of biodiesel production by transesterification— a review. *Renewable and Sustainable Energy Reviews*, 10(3), 248-268.
- Melo, C.A., Albuquerque, C., Carneiro, J., Dariva, C., Fortuny, M., Santos, A., Egues, S. & Ramos, A. (2010). Solid-Acid-Catalyzed Esterification of Oleic Acid Assisted by Microwave Heating. *Industrial & Engineering Chemistry Research*, 49 (23), 12135–12139.

- Melo, C.A., Albuquerque, C.E.R., Fortuny, M., Dariva, C., Egues, S., Santos, A.F. & Ramos, A.L.D. (2009). Use of Microwave Irradiation in the Noncatalytic Esterification of C18 Fatty Acids. *Energy & Fuels*, 23 (1), 580–585.
- Menéndez, J. A. , Arenillas, A. , Fidalgo, B. , Fernández, Y. , Zubizarreta, L. , Calvo, E. G. , & Bermúdez, J. M. (2010). Microwave heating processes involving carbon materials. *Fuel Processing Technology*, 91(1), 1-8.
- Mo, X., Lotero, E., Lu, C., Liu, Y., & Goodwin JG. (2008). A novel sulfonated carbon composite solid acid catalyst for biodiesel synthesis. *Catalysis Letters*, 123, 1–6.
- Mo, X., López, D. E. , Suwannakarn, K. , Liu, Y. , Lotero, E. , Goodwin, J. G. , & Lu, C. (2008). Activation and deactivation characteristics of sulfonated carbon catalysts. *Journal of Catalysis*, 254(2), 332-338.
- Mohammad Fauzi, A. H. , & Saidina Amin, N. A. (2013). Optimization of oleic acid esterification catalyzed by ionic liquid for green biodiesel synthesis. *Energy Conversion and Management*, 76, 818-827.
- Motasemi, F. , & Ani, F. N. (2012). A review on microwave- assisted production of biodiesel. *Renewable and Sustainable Energy Reviews*, 16 (7) , 4719- 4733.
- Niu, S. - L. , Huo, M. - J. , Lu, C. - M. , Liu, M. - Q. , & Li, H. (2014). An investigation on the catalytic capacity of dolomite in transesterification and the calculation of kinetic parameters. *Bioresource Technology*, 158, 74-80.
- Özbay, N. , Oktar, N. , & Tapan, N. A. (2008). Esterification of free fatty acids in waste cooking oils (WCO): Role of ion-exchange resins. *Fuel*, 87(10), 1789-1798.

- Park, J. - Y. , Kim, D. - K. , & Lee, J. - S. (2010). Esterification of free fatty acids using water- tolerable Amberlyst as a heterogeneous catalyst. *Bioresource Technology*, 101(1, Supplement), S62-S65.
- Park, J.Y., Wang, Z.M., Kim, D.K., & Lee, J.S. (2010). Effects of water on the esterification of free fatty acids by acid catalyts. *Renewable Energy*, 35, 614–618.
- Park, Y. - M. , Lee, J. Y. , Chung, S. - H. , Park, I. S. , Lee, S. - Y. , Kim, D. - K. , . . . Lee, K. - Y. (2010). Esterification of used vegetable oils using the heterogeneous WO₃/ ZrO₂ catalyst for production of biodiesel. *Bioresource Technology*, 101 (1), S59-S61.
- Patel, A., Brahmkhatri, V., & Singh, N. (2013). Biodiesel production by esterification of free fatty acid over sulfated zirconia. *Renewable Energy*, 51, 227–233.
- Pileidis, F. D. , Tabassum, M. , Coutts, S. , & Titirici, M. - M. (2014). Esterification of levulinic acid into ethyl levulinate catalysed by sulfonated hydrothermal carbons. *Chinese Journal of Catalysis*, 35(6), 929-936.
- Poonjarernsilp, C. , Sano, N. , & Tamon, H. (2014). Hydrothermally sulfonated single-walled carbon nanohorns for use as solid catalysts in biodiesel production by esterification of palmitic acid. *Applied Catalysis B: Environmental*, 147, 726-
- Prommuak, C. , Sereewatthanawut, I. , Pavasant, P. , Quitain, A.T. , Goto, M. , & Shotipruk, A.(2016).The Effect of Pulsed Microwave Power on Transesterification of *Chlorella* sp. for Biodiesel Production. *Chemical Engineering Communications*, 203(5), 575-580.
- Pua, F., Fang, Z., Zakaria, S., Guo, F., & Chia, C. (2011). Direct production of biodiesel from high-acid value *Jatropha* oil with solid acid catalyst derived from lignin. *Biotechnology for Biofuels*, 4, 56-63.

- Rao, K.C., Rambabu, N., Dalai, A.K., & Prasad, R.B.N. (2011). Carbon-based solid acid catalyst from de-oiled canola meal for biodiesel production. *Catalysis Communications*, 14, 20–26.
- Rashid, U., Anwar, F. , Moser, B. R., & Ashraf, S. (2008). Production of sunflower oil methyl esters by optimized alkali- catalyzed methanolysis. *Biomass and Bioenergy*, 32(12), 1202-1205.
- Rattanaphra, D. , Harvey, A. P. , Thanapimmetha, A. , & Srinophakun, P. (2011). Kinetic of myristic acid esterification with methanol in the presence of triglycerides over sulfated zirconia. *Renewable Energy*, 36(10), 2679-2686.
- Rouquerol, F. , Rouquerol, J. , Sing, K. S. W. , Maurin, G. , & Llewellyn, P. (2014). Introduction. In F. Rouquerol, J. Rouquerol, K. S. W. Sing, P. Llewellyn, & G. Maurin (Eds.) , *Adsorption by Powders and Porous Solids (Second Edition)* (pp. 1-24). Oxford: Academic Press.
- Saka, S. , & Kusdiana, D. (2001). Biodiesel fuel from rapeseed oil as prepared in supercritical methanol. *Fuel*, 80 (2) , 225- 231. doi: [https://doi.org/10.1016/S0016-2361\(00\)00083-1](https://doi.org/10.1016/S0016-2361(00)00083-1)
- Shu, Q., Nawaza, Z., Gao, J.X., Liao, Y.H., Zhanga, Q., & Wang, D.Z. (2010). Synthesis of biodiesel from waste oil feedstock and using a carbon-based solid acid catalyst: reaction and separation. *Bioresource Technology*, 101, 5374–5384.
- Shu, Q., Zhang, Q., Xu, G.H., Nawaz, Z., Wang, D.Z., & Wang. J.F. (2009). Synthesis of biodiesel from cottonseed oil and methanol using a carbon-based solid acid catalyst. *Fuel Processing Technology*, 90(7-8), 1002–1008.
- Socha, A. & Sello, J.K. (2010). Efficient conversion of triacylglycerols and fatty acids to biodiesel in a microwave reactor using metal triflate catalysts. *Organic & Biomolecular Chemistry*, 8 (20), 4753–4756.

- Son, S. M. , Kimura, H. , & Kusakabe, K. (2011). Esterification of oleic acid in a three-phase, fixed- bed reactor packed with a cation exchange resin catalyst. *Bioresource Technology*, 102(2), 2130-2132.
- Song, X., Fu, X., Zhang, C., Huang, W., Zhu, Y., & Yang, J. (2012). Preparation of a novel carbon based solid acid catalyst for biodiesel production via a sustainable route. *Catalysis Letters*, 142, 869–874.
- Souza, A. S. , dos Santos, W. N. L. , & Ferreira, S. L. C. (2005). Application of Box– Behnken design in the optimisation of an on- line pre-concentration system using knotted reactor for cadmium determination by flame atomic absorption spectrometry. *Spectrochimica Acta Part B: Atomic Spectroscopy*, 60 (5), 737-742.
- Stafiej, A. , Pyrzynska, K. , Ranz, A. , & Lankmayr, E. (2006). Screening and optimization of derivatization in heating block for the determination of aliphatic aldehydes by HPLC. *Journal of Biochemical and Biophysical Methods*, 69 (1), 15-24.
- Sunita, G. , Devassy, B. M. , Vinu, A. , Sawant, D. P. , Balasubramanian, V. V. , & Halligudi, S. B. (2008) . Synthesis of biodiesel over zirconia-supported isopoly and heteropoly tungstate catalysts. *Catalysis Communications*, 9(5), 696-702.
- Suprarukmi, D. D. , Sudrajat, B. A. , & Widayat. (2015). Kinetic Study on Esterification of Oleic Acid with Ultrasound Assisted. *Procedia Environmental Sciences*, 23, 78-85.
- Suresh Babu, C. V. , Lee, J. , Lho, D. S. , & Yoo, Y. S. (2004). Analysis of substance P in rat brain by means of immunoaffinity capture and matrix- assisted laser desorption/ ionization time- of- flight mass- spectrometry. *Journal of Chromatography B*, 807(2), 307-313.
- Tesser, R. , Di Serio, M. , Casale, L. , Sannino, L. , Ledda, M. , & Santacesaria, E. (2010). Acid exchange resins deactivation in

the esterification of free fatty acids. *Chemical Engineering Journal*, 161(1), 212-222.

Thinnakorn, K. , & Tscheikuna, J. (2014). Biodiesel production via transesterification of palm olein using sodium phosphate as a heterogeneous catalyst. *Applied Catalysis A: General*, 476, 26-33.

Titirici, M. - M. , Antonietti, M. , & Baccile, N. (2008). Hydrothermal carbon from biomass: a comparison of the local structure from poly- to monosaccharides and pentoses/hexoses. *Green Chemistry*, 10(11), 1204-1212.

Titirici, M. - M. , Funke, A. , & Kruse, A. (2015). Chapter 12 - Hydrothermal Carbonization of Biomass. In A. Pandey, T. Bhaskar, M. Stöcker, & R. K. Sukumaran (Eds.) , *Recent Advances in Thermo-Chemical Conversion of Biomass* (pp. 325-352). Boston: Elsevier.

Titirici, M. - M. , White, R. J. , Falco, C. , & Sevilla, M. (2012). Black perspectives for a green future: hydrothermal carbons for environment protection and energy storage. *Energy & Environmental Science*, 5(5), 6796-6822.

Trinh, H. , Yusup, S. , & Uemura, Y. (2018). Optimization and kinetic study of ultrasonic assisted esterification process from rubber seed oil. *Bioresource Technology*, 247, 51-57.

Trombettoni, V. , Lanari, D. , Prinsen, P. , Luque, R. , Marrocchi, A. , & Vaccaro, L. (2018). Recent advances in sulfonated resin catalysts for efficient biodiesel and bio- derived additives production. *Progress in Energy and Combustion Science*, 65, 136-162.

Veiga, P. M. , Luna, A. S. , de Figueiredo Portilho, M. , de Oliveira Veloso, C. , & Henriques, C. A. (2014) . Zn,Al- catalysts for heterogeneous biodiesel production: Basicity and process optimization. *Energy*, 75, 453-462.

- Vidal, L. , Psillakis, E. , Domini, C. E. , Grané, N. , Marken, F. , & Canals, A. (2007). An ionic liquid as a solvent for headspace single drop microextraction of chlorobenzenes from water samples. *Analytica Chimica Acta*, 584(1), 189-195.
- Vieira, S.S., Magriotis, Z.M., Santos, N.A., Saczk, A.A., Hori, C.E., & Arroyo, P.A. (2013). Biodiesel production by free fatty acid esterification using Lanthanum ($\text{La}^{3\text{p}}$) and HZSM-5 based catalysts. *Bioresource Technology*, 133, 248–255.
- Wong, Y. C., Tan, Y. P., Taufiq- Yap, Y. H. , Ramli, I. , & Tee, H. S. (2015). Biodiesel production via transesterification of palm oil by using CaO – CeO_2 mixed oxide catalysts. *Fuel*, 162, 288-293.
- Wu, K.H., Ting, T.H., Wang, G.P., Yang, C.C., & Tsai, C.W. (2008). Synthesis and microwave electromagnetic characteristics of bamboo charcoal/polyaniline composites in 2-40 GHz. *Synth Met*, 158, 688-694.
- Xie, W., & Zhao, L. (2014). Heterogeneous CaO – MoO_3 – SBA-15 catalysts for biodiesel production from soybean oil. *Energy Conversion and Management*, 79, 34-42.
- Yang, J.K., & Wu, Y.M. (1987). Relation between dielectric property and desulphurization of coal by microwaves. *Fuel*, 66, 1745-1747.
- Yao, Y., Jänis, A., & Klement, U. (2008). Characterization and dielectric properties of β -SiC nanofibres. *J Materials Science*, 43, 1094-1101.
- Ye, W., Gao, Y., Ding, H., Liu, M., Liu, S., Han, X. , & Qi, J. (2016). Kinetics of transesterification of palm oil under conventional heating and microwave irradiation, using CaO as heterogeneous catalyst. *Fuel*, 180, 574-579.

- Yoosuk, B., Udomsap, P., Puttasawat, B., & Krasae, P. (2010). Improving transesterification activity of CaO with hydration technique. *Bioresource Technology*, 101(10), 3784-3786.
- Yusà, V., Pardo, O., Pastor, A., & de la Guardia, M. (2006). Optimization of a microwave- assisted extraction large- volume injection and gas chromatography- ion trap mass spectrometry procedure for the determination of polybrominated diphenyl ethers, polybrominated biphenyls and polychlorinated naphthalenes in sediments. *Analytica Chimica Acta*, 557(1), 304-313.
- Zatta, L., Gardolinski, J. E. F. d. C., & Wypych, F. (2011). Raw halloysite as reusable heterogeneous catalyst for esterification of lauric acid. *Applied Clay Science*, 51(1), 165-169.
- Zhang, D. - Y., Duan, M. - H., Yao, X. - H., Fu, Y. - J., & Zu, Y. - G. (2016). Preparation of a novel cellulose- based immobilized heteropoly acid system and its application on the biodiesel production. *Fuel*, 172, 293-300.
- Zhang, H., Ding, J., & Zhao, Z. (2012). Microwave assisted esterification of acidified oil from waste cooking oil by CERP/ PES catalytic membrane for biodiesel production. *Bioresource Technology*, 123, 72-77.
- Zhang, L., & Zhu, H. (2009). Dielectric, magnetic, and microwave absorbing properties of multi-walled carbon nanotubes filled with Sm₂O₃ nanoparticles. *Materials Letters*, 63, 272-274.
- Zhang, Q., Saleh, A. S. M., Chen, J., & Shen, Q. (2012). Chemical alterations taken place during deep- fat frying based on certain reaction products: A review. *Chemistry and Physics of Lipids*, 165(6), 662-681.
- Zhang, Y., Wong, W.T., & Yung, K.F. (2014). Biodiesel production via esterification of oleic acid catalyzed by chlorosulfonic acid modified

zirconia. *Applied Energy*, 116, 191–198.

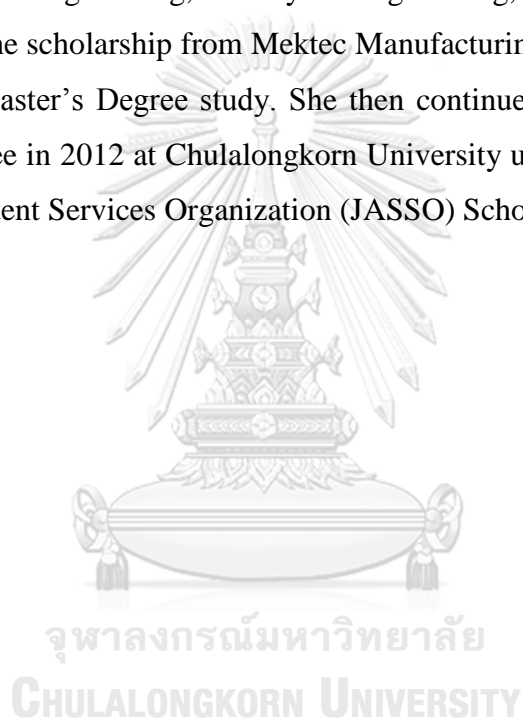
Zougagh, M., Garcia de Torres, A., Vereda Alonso, E. , & Cano Pavón, J. M. (2004). Automatic on line preconcentration and determination of lead in water by ICP-AES using a TS-microcolumn. *Talanta*, 62(3), 503-510.

Zullaikah, S., Lai, C. - C. , Vali, S. R. , & Ju, Y. - H. (2005) . A two- step acid- catalyzed process for the production of biodiesel from rice bran oil. *Bioresource Technology*, 96(17), 1889-1896.



VITA

Miss Laddawan Tumkot was born on the 25th of April 1987, in Udon Thani, Thailand. She earned a Bachelor of Engineering Degree in Chemical Engineering from Department of Chemical Engineering, King Mongkut's University of Technology Thonburi (KMUTT) in April 2009. During senior project work, she received financial support from Thailand Research Fund (TRF) through the Industrial and Research Projects for Undergraduate Students (IRPUS). She holds a Master's degree in Chemical Engineering, Faculty of Engineering, Chulalongkorn University in 2011. She got the scholarship from Mektec Manufacturing Corporation (Thailand) Ltd. during her Master's Degree study. She then continued to pursue her Doctor of Engineering Degree in 2012 at Chulalongkorn University under the 60/40 scholarship and the Japan Student Services Organization (JASSO) Scholarship.



REFERENCES



จุฬาลงกรณ์มหาวิทยาลัย
CHULALONGKORN UNIVERSITY



จุฬาลงกรณ์มหาวิทยาลัย
CHULALONGKORN UNIVERSITY

VITA

NAME Laddawan Tumkot
DATE OF BIRTH April 25th, 1987
PLACE OF BIRTH Udon Thani



จุฬาลงกรณ์มหาวิทยาลัย
CHULALONGKORN UNIVERSITY